onto a brass mount. A few drops of isopropanol were applied to assist adherence of the grains, and the mount was vacuum dried in a desiccator. The dry sample was coated with a conductive layer of Pt, since this was not expected to interfere significantly with predicted components of the sample. Samples were subjected to accelerating voltage ranging from 2 to 15 kV, depending on the competing needs of high resolution and reasonably comprehensive semi-quantitative analytical data. The IFESEM was fitted with a thin window EDS detector capable of identifying all elements down to and including Li.

Leach tests

Introduction

Two single-stage leach tests with water and dilute sulphuric acid were designed to help assess the likely hydrogeochemical consequences of flushing sulphidic tailings sediments with rain, river or harbour water. A third single-stage extraction test with ammonium acetate was conducted to determine the concentration of metals adsorbed onto grain surfaces. The presence and apparent reactivity of silicate slag in many samples suggested that conventional sequential extraction tests would be of limited use, since the behaviour of variably altered slag in a range of extraction media is unknown. This conclusion appears to be supported by the results. Samples from saturated and unsaturated settings were chosen and submitted to Amdel (Melbourne).

Deionised water and dilute sulphuric acid

Twenty gram portions of tailings material from each sample were mixed separately with distilled/deionised water and 0.01 M sulphuric acid (pH ≈2.0) in a solid:fluid weight ratio of 1:2. The mixtures were gently agitated continuously for 48 hours. The leachate was removed from contact with the sediment, filtered through a 0.45 μm filter and analysed for Cu, Fe, Mn, Al, Si, As, Sn, Mo, Cr, Zn, Cd, Pb, Ba, Co, B, V, Ag, La, Ni, Y and Sr by ICP-ES with detection limits of 0.01 μg/L. Sulphate was analysed by Ion Chromatography. The pH and EC of the leachate was measured five minutes after initial mixing, after 1 and 2 hours, and thereafter on a regular basis.

Ammonium acetate

Five gram batches of tailings material from each sample were added to 1.0 M ammonium acetate (NH_4OAc) solution in a solid:fluid weight ratio of 1:10 (Kersten & Forstner 1989). Gentle agitation of the mixtures was continuous for 24 hours. The leachate was filtered through a 0.45 μm filter and analysed for Cu, Fe, Mn, Al, Si, As, Sn, Mo, Cr, Zn, Cd, Pb, Ba, Co, B, V, Ag, La, Ni, Y and Sr by ICP-ES with detection limits of 0.01 μg/L. Sulphate was measured by Ion Chromatography. The pH, EC and Eh of the leachate was measured five minutes after initial mixing, after 15 minutes, and at 2 hour intervals thereafter.

5 Results

5.1 General

Most recent studies of tailings focus on engineered impoundments, and direct comparison between hydrogeochemical processes in such settings and in an active fluvial-deltaic system is difficult. Tailings from the Mount Lyell copper mine are subject to relatively unique processes, such as short and medium-term cyclical drying/wetting, flushing, oxidation, nutrient addition and bacterial modification.

The redox interface between largely oxidised and largely unoxidised sulphidic tailings material is difficult to locate in the field, and appears to have little direct relationship with the current water table. This can be attributed to the following factors:

- Fresh sulphidic material, highly oxidised tailings and original sediments are often similarly coated with orange, secondary iron-oxides, and hence display an oxidised appearance.
- Long-term changes in groundwater levels are predicted to have resulted from factors such as operation of the John Butters Power Station, thereby disrupting pre-existing groundwater levels.
- Seasonal, tidal and dam-related river level fluctuations result in significant short-term changes in groundwater levels.
- The sporadic distribution of organic matter and associated anaerobic bacterial activity often results in sulphide precipitation in previously oxidised zones.

For the purposes of this report the tailings will be referred to as either saturated or unsaturated, rather than oxidised and unoxidised. While river bed sediments are essentially always saturated, tailings in the banks and delta may be broadly divided into saturated and unsaturated zones. During the winter months, much of the unsaturated tailings are likely to be permanently moist. The classification of tailings based on pore water content is complicated by perched water tables which result from discontinuous clay-rich horizons at various levels in both the sediment banks and delta. The clay layers permit sufficient water to be retained in overlying sediments to prevent significant oxidation of pyrite locally. Plate 6 displays an example of this phenomenon on Bank H. Largely fresh sulphidic material is visible at more than 1.5 m above the present water table, and is surrounded on all sides by sulphide depleted sediment.

Crusted portions of the tailings deposits are believed to represent coarser grained accumulations that have been cemented by metal-oxide rich precipitates. While most surficial tailings deposits display metal-oxide bearing coatings, a coarser grain size appears to facilitate local lithification by oxides. The distribution of both small and large crusted sections of tailings in both the sediment bank deposits and delta confirms this observation. For example, crusts often develop in the downstream shadows of dead trees/logs on sediment banks, and log jams/vegetation on the delta. Such objects cause localised low-energy zones which facilitate the deposition of relatively coarse grained sediment.

Morphology and geology of the delta

The subaerial King River delta consists of a broad expanse of low relief, highly oxidised tailings material with irregularly distributed and partially buried logs and occasional anthropogenic waste (plates 1, 5 and 6). The delta displays a maximum relief of approximately 2.0 m above the harbour water during an average low tide, but the majority exhibits relief of less than 1.0 m. Typical tidal variations produce vertical water level rises in the order of 30 to 50 cm, and under low tide conditions the subaerial surface area of the delta is approximately 2.5 km^2. Anecdotal evidence indicates that rises in water level up to approximately 1.0 m may occur more than once per year. During these peak flow events, much of the delta is inundated.

The delta is bisected by a narrow channel through which the King River flows (figure 2), and quasi-perennial and shallow ephemeral channels traverse the surface of both the north and south lobes. These lesser waterways are instrumental in conveying overflowing river water and incident rainfall off the delta toward the harbour.

Plate 5 Hand-held sonic drilling equipment deployed on the north lobe of the delta for the installation of DEL-C1. The view is to the south-east towards Macquarie Harbour.

Plate 6 Vertical profile through part of the unsaturated zone in Bank H along the edge of the King River. The relatively unoxidised blue-green material is discontinuous in all directions. Oxidation was probably retarded by the local retention of perched groundwater above a clay-rich horizon.

The north and south lobes of the delta appear to display broadly different physical and, therefore, chemical characteristics. In general terms the north lobe is comprised of finer grained material than the south, and therefore includes a higher proportion of finer grained sand, clay and organic debris. The physical differences in the delta deposits may be attributed to the relative energetics of lateral transport of sediment at the head of the developing delta. The north lobe of the delta appears to be more sheltered in terms of lateral transport than the south lobe, and hence finer grained fractions have a greater opportunity to settle out. These gross physical and chemical differences in the sediment are reflected in the groundwater chemistry (see below).

Large sections of the delta, in particular the southern lobe, appear to have accumulated by progressive development during flood events (plate 7), and these deposits appear to control its gross structure. These foresets display current directions radiating away from the mouth of the King River. Highly irregular relief comprising chaotically distributed megascopic foresets established during peak flow will be sporadically filled with finer grained, horizontally stratified components during the waning phase of a flood event. Successive flood events will remove portions of the earlier deposits. Consequently, the detailed internal structure of the delta is predicted to be extremely complex and locally highly variable in terms of grain size, composition and the orientation, scale and anisotropy of internal layering. A widespread distinctive laminated horizon identified by EGI (1991c) was not confirmed by this study and, although coherent horizontal stratification is sometimes evident on the scale of metres (especially on the north lobe), it is considered unlikely to be more continuous.

In addition to typical silicate- and sulphide-bearing tailings sediment, the delta contains a small but common component of slag, numerous thin layers (<1 to 30 mm) of leaf-litter dominated organic debris, irregularly distributed buried and exposed logs, and a minor component of miscellaneous refuse (eg tyres, cardboard, cans and bottles). Animal bones are not uncommon, and occasionally display a thin surficial green precipitate that appears to be malachite (copper carbonate).

Wind erosion is reportedly significant during the dry summer months, and small aeolian dunes at the back of the north lobe are evidence of this effect. The dunes indicate that wind-borne tailings transport is dominantly to the east. Widespread evaporative crusts developed in local depressions on top of the delta would have the effect of minimising wind-borne transport of tailings and acid-forming material, but significant quantities of unconsolidated surficial sand could be mobilised. The effect of the evaporative crust on retarding recharge to the delta from precipitation is unknown, but could be significant.

Morphology and geology of river banks

The majority of sediment contained in the King River overbank deposits is unsaturated, extensively oxidised and comprised largely of mine tailings. Based on field and petrographic evidence, the grain size of tailings material appears to increase downstream, with the delta hosting the coarsest grained debris.

Excavations in the downstream end of Bank M (Locher 1995, photos 4.7 and 4.8) revealed that the sediment banks have a strongly layered internal structure resembling a broad, open antiform, with its axis running along the central portion of the bank. These deposits appear to have evolved by progressive draping of sediment onto this geometry. Although lateral continuity of layers for more than tens of metres is unlikely, well developed stratification and shallow dips away from the spine of the bank are predicted to be common features. The downstream ends of each of the four banks examined in this project were distinctly rich in clay, and this is likely to be a common feature of all such deposits.

Puddles, ponds, small lagoons, creeks and swampy ground characterise the landward side of many sediment bank deposits (plates 8 and 9). These areas often develop permanent or intermittent creeks, and contain highly acid to near neutral flows, depending on local catchments and the internal structure of the banks. Given the moderate to high hydraulic conductivity of the tailings material and relatively low water table, semi-permanent bodies of water situated *on* the banks (eg Bank H) are direct evidence of (shallow) subsurface aquitards (ie clay dominated layers). Preliminary observations suggest that the internal structure of the banks has significant implications for surface runoff and groundwater discharge, and may exacerbate the rapid release of acid and metals. For instance, the geometry of near-surface clay horizons acts to preclude the deep penetration of some precipitation. These discontinuous aquitards permit partial infiltration and then facilitate rapid discharge and accumulation of incident rainfall to shallow pools on the banks. Subsequent evaporation and concentration of acid and metals is likely to be common prior to a surface flushing event which will deliver short-lived but high-volume pulses of acidic surface leachate to the receiving environment (plate 10).

Organic debris comprising buried logs and abundant leaf litter is irregularly distributed throughout the banks. Drilling on Banks R and H encountered large logs at several metres depth, and required relocation of piezometers.

Field observations indicate that release of acid and metals from delta and banks will be in the form of quasi-continuous seepage from the saturated tailings accumulations and periodic surficial flushing by rainfall events. The short-term storm/flood runoff events could be producing the most damaging ecological impacts through punctuated release of accumulated/concentrated acid and metals from the surface of the banks and delta.

King River – bottom sediments

River bottom sediments provided by Locher (1995, Project 4, map 5) reveal a predominance of slag and coarse grained sulphidic sediments. The relatively high density of this material has restricted its distribution to the river bottom and the upper portion of the delta. Since the disposal of slag only commenced in 1972, much of it resides in the upper part of the river bottom sequence (Locher 1995), and the upper 2 m of the delta.

The occurrence of the slag-rich tailings appears to be fundamental to the formation of the 'hardpan' in the base of the King River, and similar cementation processes in other crusted tailings material.

Microbial activity

Carpenter et al (1991) identified significant populations of anaerobic bacteria in harbour sediments near the mouth of the King River, and reported that these contained biomarkers indicating the presence of sulphate reducing bacteria. Gaseous emissions from numerous small point sources were observed on both lobes of the delta (particularly the north) in the tidal interface zone (plate 11). Field-based flame tests indicated the presence of methane at a few of these sites. This suggests that methanogenic bacteria are flourishing locally at least.

A strong odour of H_2S was detected in groundwater samples on Banks N and H, from the tidal zone of the south lobe of the delta and from relatively acid groundwater samples. This gas is likely to have been generated by sulphate reducing bacteria. Elevated concentrations of

Plate 7 View from the south lobe of the delta looking north-east towards the King River. The typical surface expression of foresets is evident in the foreground. The slight relief of this material is due to partial cementation by iron-oxides.

Plate 8 View looking up the King River at a semi-permanent channel on the landward side of the crest of Bank H. Since groundwater levels in this bank are 2 to 3 m lower than the surface, the ponded water confirms the presence of near-surface aquitards (ie clay horizons). The water in this channel is highly acidic (pH ≈3.0) and contains abundant iron-stained filamentous algae.

Plate 9 Fresh sulphidic tailings on the surface of Bank D overlying more oxidised sediment. Ponded water on the bank indicates the occurrence of near-surface clay layers.

Plate 10 View of the downstream end of Bank H during a period of heavy rainfall. Ponded surface water evident in plate 8 is being flushed into the river and creating the orange acidic-plume. The green colour of the bank here is due to a localised deposit of fresh sulphuric tailings.

HS^- are also predicted to be present in other less acid water which is associated with subsurface organic debris and microbial activity. The anomalously low aqueous sulphate concentrations (representing total soluble sulphur) in groundwater samples DEL-WS1, DEL-WD1 and DEL-WS2 are interpreted to reflect microbial sulphate reduction, and pyrite precipitation. Five day biochemical oxygen demand analyses ($BOD_{(5)}$) of relatively reduced groundwater from DEL-WS1 and DEL-WS2 returned results of 21 mg/L and 8 mg/L respectively, supporting the presence of significant bacterial activity.

In the delta, the distribution of subsurface organic debris (leaf litter, wood debris and organic refuse) is highly irregular, and varies laterally on the scale of metres, and vertically on the scale of centimetres. The distribution of subaqueous organic material appears to have a fundamental control on bacterial activity and therefore on groundwater chemistry. Based on the distribution of ultra fine grained biogenic pyrite (framboids) in the delta, sulphate reducing bacteria appear to be widespread proximal to subaqueous organic debris. With more organic debris in the north lobe, the groundwater chemistry is generally less acid, and aqueous metal concentrations are generally lower, particularly in the tidal interface zone where sediments are permanently saturated. Biogenic pyrite was also observed on subaqueous organic debris in the sediment banks.

Physical disruption of saturated tailings (eg excavating, auguring, drilling and installing piezometers) often resulted in the visible release of biogenic pyrite to the water column. Almost complete oxidation of such biogenic pyrite over a period of a few days is believed to be responsible for significant variations between field and laboratory pH and conductivity measurements in some of the relatively reduced, unfiltered/unacidified groundwater samples. Laboratory pH measurements were more acid, EC measurements were higher, and yet dissolved iron concentrations were dominated by ferrous iron. These results indicate that the oxidation of ferrous to ferric iron was not responsible for these changes, and that the dissolution of some acid producing component was implicated.

From these observations we can conclude that natural bioremediation is currently active in both the banks and the delta, and is at least locally very effective in lowering the concentrations of acid and metals in groundwater.

Pyrite oxidation rate

Relatively rare, thin blankets (1 to 20 cm) of fresh sulphide-rich tailings are irregularly distributed over the lower portions of some banks and parts of the north lobe proximal to the river. Their distribution indicates that deposition occurred after the dam became operational and the mine was closed. It is concluded that they represent river bottom sediments that have been remobilised during peak flow events (ie 1 to 2 times/year). Anecdotal evidence indicates that the most recent of such events occurred during August to September 1994. This suggests that significant oxidation of pyritic tailings material takes more than 12 months.

Trace amounts of detrital pyrite trapped in standing dead trees, preserved by the moist, reducing conditions, have been observed on Bank R at a level that indicates pre-dam flood transport. Since negligible deposition or erosion of tailings from the top or landward side of Bank R is indicated since operation of the John Butters Power Station, and petrographic work indicates little or no fresh pyrite remains on the surface of this sediment bank, it would appear that virtually complete oxidation has taken less than four years.

To assist evaluation of pyrite oxidation rates fresh samples of pyrite-rich tailings taken from the river edge of the downstream end of Bank N have been placed on top of the bank in depressions in large logs as well as in plastic containers with porous bases at the beginning of August 1995.

5.2 Hydrology

The banks and delta receive an average annual rainfall of 1800 to 2200 mm (figure 22). Runoff plus infiltration for the banks and delta is predicted to be close to 70 to 80%, with a recharge estimated at about 20%. Evapotranspiration will be negligible at present, but may be locally as high as 10%. Some proportion of the runoff and infiltration is ponded on the surface of the banks and delta, and is concentrated by evaporation.

Groundwater in the delta appears to be derived from on-shore groundwater sources, and from surface infiltration by rain, river and harbour water. The majority of the delta exhibits less than 1.5 m of relief relative to the median harbour water level, and depth to groundwater in the delta is usually less than 50 cm. Groundwater levels respond rapidly to rainfall, tidal influences and river level changes caused by operation of the John Butters Power Station. Proximal to the tidal interface zone the direction of the hydraulic gradient depends on tidal conditions, and significant variations in river flow conditions are predicted to have a similar effect. Significant seepage from the delta can be observed in the tidal zone at low tide, and groundwater reacts with the atmosphere to produce what are likely to be iron-bearing precipitates (plate 12).

Groundwater in the sediment banks appears to be derived primarily from infiltration by rainfall and from surface drainage, with lesser contributions from river-margin groundwater sources and local input from the King River. Extensive groundwater seepage from the banks during low flow conditions is evident in photo 5.5 from Locher (1995).

5.3 Dimensions of tailings deposits

Photographic enlargements of the sediment banks and delta were prepared from Tasmap's 1988 colour aerial photographic coverage of the central west coast of Tasmania. The principal photographs were from Run 26W, frames 1123-144 and 1123-145 at an initial scale of 1:42 000. Black and white scaled enlargements were scanned and the digital images analysed to establish the area and perimeter of individual tailings deposits. Field measurements along selected banks and the delta using a chain were conducted to minimise errors introduced by photographic edge distortions. Image analysis determinations of the surface area of each bank and the delta, and the perimeter of each deposit along the King River or Macquarie Harbour are provided in table 2.

The maximum depth of tailings material in each of the banks studied was determined from a combination of geological logging (auger and drill samples), petrographic work and bulk chemical analysis of sediment samples. When compared with visual techniques, the total Cu, S, Fe and As content of tailings samples appeared to provide a reasonable indication of the origin of the sedimentary material. When visual evaluation was unreliable, the bulk analysis was used to indicate a sample's origin. The following values generally provided a reliable indication of tailings-free sedimentary material: Cu $\leq$50 ppm, S $\leq$500 ppm, Fe $\leq$1.5%, and As $<$3 ppm.

Volumetric estimates of tailings contained in each surveyed bank were calculated on the maximum depth of tailings as determined from drillhole or piezometer sediment sample chemistry (ie surface area x max. depth of tailings). Values for the maximum depth of tailings in unsurveyed banks were interpolated from available data. Tonnages of tailings contained in the sediment banks are based on a specific gravity of 1.6 for unsaturated material as determined by Locher (1995). Results are provided in table 2.

Plate 11 View of the discrete occurrence of a gaseous emission from the delta. The small vent is highlighted by the presence of a concentration of bubbles. This plate was taken on the north lobe of the delta at the tidal interface zone. Flame tests indicated the presence of methane at some of these sites.

Plate 12 Groundwater seepage along the tidal zone on the north lobe of the delta. Reaction of the groundwater with air produces an iridescent precipitate on the surface of the water (?iron-oxide).

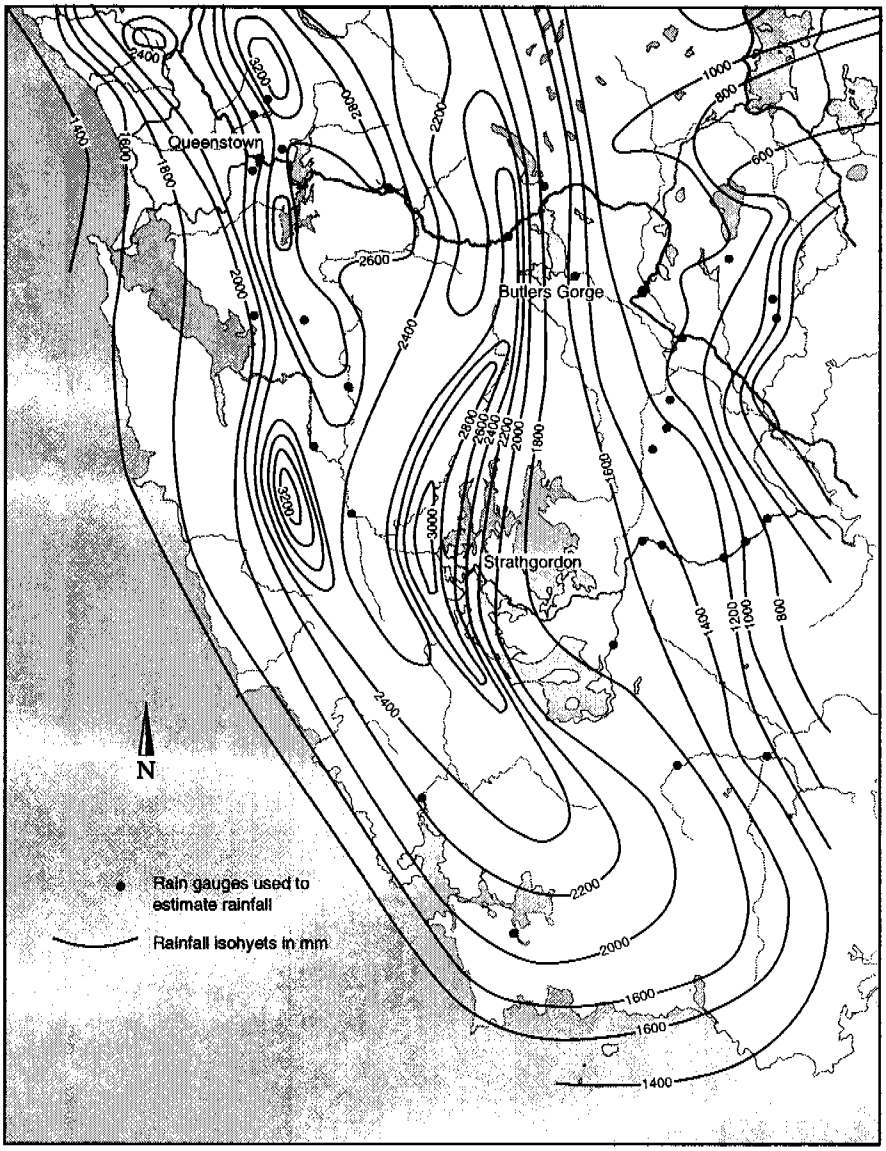

Figure 22 Regional annual rainfall for the study area

5.4 Analytical data

Hydrogeochemistry

Analyses of groundwater and surface-water samples indicate that several elements have the potential to contribute to ecological problems. These primarily include Cu, Fe, Mn, Al, Si, As, Ni, Zn, Hg, Se, Pb and Co. Analytical results are provided in table 3. The concentrations of key metals in groundwater in the sediment banks and delta are roughly an order of magnitude lower than those in surface drainage from the lease site. However, they are roughly an order of magnitude higher than those measured in the lower King River (MLMRCL data from sites 28 and 29, see figure 23) in 1993 and 1994.

Aqueous copper concentrations range from below detection limit (BDL) for near neutral groundwater samples from the tidal interface zone on the delta, to a maximum of 8.7 mg/L in highly acidic groundwater from Bank D. Aqueous Cu concentrations in the sediment banks generally increase down the river, with groundwater in the topographically lower banks and river margin of the delta hosting the highest concentrations.

Table 2 Dimensions of tailings deposits

Location	Subaerial Surface Area (sq. m)	Perimeter Along River Bank (m)	Perimeter Along Harbour (m)	Average Depth of Tailings (m)	Volume of Tailings (m3)	Specific Gravity	Mass of Tailings (Tonnes)
Bank A	24600	686		0.5	1.23E+04	1.6	1.97E+04
Bank B	26100	1128		1.3	3.39E+04	1.6	5.43E+04
Bank C	11950	361		2.5	2.99E+04	1.6	4.78E+04
Bank D	39525	925		3	1.19E+05	1.6	1.90E+05
Bank E	17150	505		3.5	6.00E+04	1.6	9.60E+04
Bank F	26875	652		4	1.08E+05	1.6	1.72E+05
Bank G	17250	660		4.5	7.76E+04	1.6	1.24E+05
Bank H	21900	679		4.9	1.07E+05	1.6	1.72E+05
Bank I	2125	153		5	1.06E+04	1.6	1.70E+04
Bank J	10925	503		5	5.46E+04	1.6	8.74E+04
Bank K	4325	243		5	2.16E+04	1.6	3.46E+04
Bank L	25725	689		5	1.29E+05	1.6	2.06E+05
Bank M	27225	606		5	1.36E+05	1.6	2.18E+05
Bank N	34150	501		5	1.71E+05	1.6	2.73E+05
Bank O	24400	699		5	1.22E+05	1.6	1.95E+05
Bank P	17450	379		5.2	9.07E+04	1.6	1.45E+05
Bank Q	32150	634		5.4	1.74E+05	1.6	2.78E+05
Bank R	46050	763		5.4	2.49E+05	1.6	3.98E+05
Delta North	977000	1393	1564				
Delta South	1050000	1515	2239				
Delta Island	57500	1073					
TOTAL	**2.49E+06**	**14747**	**3803**		**1.70E+06**		**2.73E+06**

Analytical differences between filtered and unfiltered water samples suggest that Cu is partially particulate (ie >0.45μm) and partly dissolved (ie <0.45μm). Iron in groundwater samples is almost totally soluble, and elevated concentrations (0.2 to ≈18.0 mg/L) are widespread in the delta and sediment bank deposits. These concentrations are dominated by ferrous species.

Silicon is largely soluble in groundwater samples, and dissolved concentrations range from 0.9 to 78 mg/L, with a majority of samples biased toward the higher concentrations. Concentrations of Al are relatively high under acidic conditions, and range from BDL to ≈23 mg/L. Despite locally high clay fractions in some tailings samples, there is little difference in Al concentrations between filtered and unfiltered samples. Aqueous Mn ranges from 0.5 to 22 mg/L, with most groundwater samples containing relatively high concentrations. Manganese also appears to be almost exclusively in soluble form.

Concentrations of soluble As range from BDL to 0.33 mg/L, but are commonly near the upper value in both the delta and sediment bank deposits. While the As is sometimes largely particulate, in other samples it is dominantly soluble. Arsenic values are often several times higher than ANZECC guidelines for the protection of aquatic ecosystems. Soluble Ni concentrations in groundwater are sporadically elevated, and range from BDL to 1.02 mg/L. Nickel is dominantly in soluble form in water samples. Aqueous Zn concentrations are relatively high in the sediment banks deposits and acidic delta samples, and range from BDL to 5.03 mg/L. Zinc is largely in a soluble form in groundwater samples. Cadmium

Table 3 Groundwater and surface-water chemistry – analytical results

Sample Number	Na (mg/l)	K (mg/l)	Ca (mg/l)	Mg (mg/l)	Cl (mg/l)	Sulphate (mg/l)	P (mg/l)	Nitrate (mg/l)	Bi-carbonate (mg/l)	As (mg/l)	Sn (mg/l)	Mo (mg/l)	Cr (mg/l)	Zn (mg/l)	Cd (mg/l)	Pb (mg/l)	Ba (mg/l)	Co (mg/l)	Fe (mg/l)	B (mg/l)	Si (mg/l)
DEL-WS1-UU								< 0.01	19	0.04	0.06	<0.01	<0.01	0.01	<0.01	<0.01	10.23	<0.01	17.42	0.83	25.73
DEL-WS1-AF	1941.41	39.60	113.13	441.41	4148.48	408.08	<0.01			0.23	0.05	<0.01	<0.01	0.03	<0.01	<0.01	14.30	<0.01	17.50	0.82	27.24
DEL-WD1-UU								5.01	9												
DEL-WD1-AF	1891.92	51.21	123.23	498.99	4422.22	22.22	0.20			0.08	0.06	<0.01	<0.01	0.02	<0.01	0.06	32.74	<0.01	17.95	0.72	25.63
DEL-WS2-UU								11.84	87	0.20	0.10	0.05	<0.01	<0.01	<0.01	21.00	10.03	<0.01	0.20	1.83	18.81
DEL-WS2-AF	1882.83	245.45	210.10	1196.97	9848.48	188.89	<0.01			0.01	0.10	0.06	<0.01	0.02	<0.01	<0.01	9.28	<0.01	0.27	1.78	19.19
DEL-WS3-UU								< 0.01	< 1												
DEL-WS3-AF	1449.49	5.25	265.66	482.83	2723.23	4914.14	<0.01			<0.01	0.13	<0.01	<0.01	0.11	0.08	0.11	0.76	<0.01	14.35	2.39	28.54
DEL-WS4-UU								1.64	< 1												
DEL-WS4-AF	368.69	<0.01	207.07	264.65	975.76	6434.34	<0.01			0.20	0.07	<0.01	<0.01	0.19	0.13	0.17	0.66	<0.01	11.89	4.01	31.93
DEL-WS5-UU								< 0.01	< 1												
DEL-WS5-AF	223.23	<0.01	65.66	107.07	309.09	3328.28	<0.01			<0.01	0.04	<0.01	<0.01	0.17	0.02	<0.01	0.37	0.33	16.20	1.03	28.01
DEL-WS6-UU								0.51	< 1												
DEL-WS6-AF	574.75	8.59	137.37	267.68	876.77	4059.60	<0.01			<0.01	0.02	<0.01	<0.01	0.09	0.04	0.01	0.50	<0.01	16.29	1.05	20.36
DEL-WS7-UU								< 0.01	< 1												
DEL-WS7-AF	239.39	<0.01	129.29	143.43	521.21	4259.60	<0.01			0.07	<0.01	<0.01	<0.01	0.08	0.06	0.06	0.43	<0.01	15.37	1.69	25.51
DEL-WS8-UU								< 0.01	< 1	0.31	<0.01	<0.01	<0.01	0.57	0.03	0.10	0.42	<0.01	16.54	0.74	27.37
DEL-WS8-AF	349.49	4.34	137.37	230.30	746.46	2701.01	<0.01			0.02	0.07	<0.01	<0.01	0.07	0.04	0.07	0.67	<0.01	16.23	1.06	29.96
DEL-WS9-UU								< 0.01	< 1	0.11	0.02	<0.01	<0.01	0.95	<0.01	0.02	0.26	0.31	17.42	0.09	56.15
DEL-WS9-AF	7.17	<0.01	46.46	18.79	141.41	2036.36				0.00	<0.01	<0.01	<0.01	0.91	0.02	<0.01	0.46	0.11	17.26	0.35	55.41
DEL-WS1-0UU								< 0.01	< 1												
DEL-WS10-AF	11.41	<0.01	42.42	15.76	542.42	2139.39				0.01	0.03	<0.01	<0.01	1.28	0.02	0.04	0.31	0.22	17.19	0.36	67.18
DEL-WS11-UU	26.60	<0.01	108.00	52.30	84.40	1902.00		23.6	< 1	0.05	0.08	<0.01	<0.01	1.81	0.03	0.03	0.28	2.10	20.60	0.81	55.10
DEL-WS11-UU/F										<0.01	0.09	<0.01	<0.01	2.01	0.02	0.08	0.15	1.90	16.30	0.57	47.96
DEL-WS12-UU								< 0.01	< 1												
DEL-WS12-AF	649.49	8.79	111.11	280.81	1235.35	2642.42				<0.01	0.07	<0.01	<0.01	0.65	0.02	0.02	0.54	0.10	17.11	0.47	26.21
DEL-WD12-UU								< 0.01	1												
DEL-WD12-AF	706.06	26.57	270.71	379.80	1284.85	2023.23				0.33	0.02	<0.01	<0.01	0.06	0.02	<0.01	1.01	<0.01	17.09	0.62	40.60
DEL-WS13-UU								< 0.01	< 1												
DEL-WS13-AF	121.21	<0.01	69.70	79.70	318.18	2692.93				0.18	0.05	<0.01	<0.01	0.34	0.02	<0.01	0.51	0.08	16.89	0.53	38.81
DEL-WS14-UU								< 0.01	< 1												
DEL-WS14-AF	169.70	<0.01	142.42	182.83	277.78	3752.53				0.00	0.07	<0.01	<0.01	1.10	0.04	0.02	0.53	0.83	16.09	1.04	45.75
DEL-WS15-UU								< 0.01	< 1	0.29	<0.01	<0.01	<0.01	0.04	0.02	<0.01	1.13	<0.01	16.94	0.59	17.59
DEL-WS15-AF	1379.80	35.76	221.21	422.22	2750.51	2802.02				0.10	<0.01	<0.01	<0.01	0.06	0.01	<0.01	1.06	<0.01	16.55	0.90	20.49
DEL-WS16-UU	302.00	14.40	71.00	122.30	545.00	255.00		< 0.01	8	0.07	0.04	0.03	<0.01	<0.01	<0.01	0.02	5.44	<0.01	0.48	0.09	27.13
DEL-WS16-UU/F										0.04	0.08	<0.01	0.01	<0.01	<0.01	<0.01	4.07	<0.01	0.11	0.11	26.42
DEL-WS17-UU								< 0.01	< 1	0.22	<0.01	<0.01	<0.01	5.03	0.03	0.02	0.12	0.69	17.05	0.34	77.89
DEL-WS17-AF	6.36	<0.01	59.60	36.57	134.34	2463.64				0.22	0.03	<0.01	<0.01	4.88	0.04	0.04	0.27	0.50	16.67	0.69	74.42
DEL-WS22-UU	1859.00	309.60	17.70	1223.00	8030.00	186.00		< 0.01	75	0.32	0.16	0.04	<0.01	<0.01	<0.01	<0.01	10.21	<0.01	0.17	2.08	18.68
DEL-WS22-UU/F										0.14	0.24	0.01	<0.01	<0.01	<0.01	0.01	4.83	<0.01	0.04	1.74	17.20
DEL-WS25-UU	1868.00	150.10	194.00	667.40	10106.00	34.00		565.1	< 1	0.11	<0.01	<0.01	<0.01	0.04	<0.01	<0.01	0.37	0.02	1.41	1.69	2.68

Table 3 (continued) Groundwater and surface-water chemistry – analytical results

Sample Number	Mn (mg/l)	V (mg/l)	Cu (mg/l)	Ag (mg/l)	La (mg/l)	Ni (mg/l)	Y (mg/l)	Al (mg/l)	Sr (mg/l)	Se (µg/l)	Sb (µg/l)	Tl (µg/l)	Hg (µg/l)	Comments
DEL-WS1-UU	5.00	<0.01	<0.01	<0.01	<0.01	<0.01	<0.01	0.24	1.39					
DEL-WS1-AF	5.09	<0.01	<0.01	<0.01	<0.01	0.03	<0.01	0.16	1.40					
DEL-WD1-UU														
DEL-WD1-AF	5.08	<0.01	<0.01	<0.01	<0.01	0.04	<0.01	0.32	1.67					
DEL-WS2-UU	1.80	<0.01	<0.01	<0.01	<0.01	0.01	<0.01	0.46	3.13					
DEL-WS2-AF	2.07	<0.01	<0.01	<0.01	<0.01	0.03	<0.01	0.53	3.23	107.07	1.21	3.33	<0.01	
DEL-WS3-UU														
DEL-WS3-AF	22.29	0.09	<0.01	<0.01	0.07	<0.01	<0.01	0.38	1.31					
DEL-WS4-UU														
DEL-WS4-AF	23.07	0.16	<0.01	<0.01	0.13	<0.01	<0.01	<0.01	0.84					
DEL-WS5-UU														
DEL-WS5-AF	18.97	0.04	<0.01	<0.01	0.03	0.01	<0.01	0.23	0.23					
DEL-WS6-UU														
DEL-WS6-AF	13.82	0.03	<0.01	<0.01	0.03	0.04	<0.01	0.07	0.79					
DEL-WS7-UU														
DEL-WS7-AF	22.20	0.05	<0.01	<0.01	0.04	0.02	<0.01	0.02	0.46					
DEL-WS8-UU	21.97	0.02	0.43	<0.01	0.01	<0.01	<0.01	0.79	1.11					
DEL-WS8-AF	22.19	0.03	<0.01	<0.01	0.04	0.01	<0.01	0.63	1.09	8.18	0.30	0.91	<0.01	
DEL-WS9-UU	8.62	<0.01	3.25	<0.01	0.01	0.05	<0.01	2.58	0.16					
DEL-WS9-AF	8.80	0.01	1.14	<0.01	0.02	0.06	<0.01	0.97	0.18	0.30	0.10	<0.01	0.20	
DEL-WS1-0UU														
DEL-WS10-AF	6.53	0.01	8.40	<0.01	0.04	0.03	0.02	9.00	0.16					
DEL-WS11-UU	23.00	0.04	0.35	<0.01	0.03	0.17	<0.01	0.90	0.46					
DEL-WS11-UU/F	23.07	0.03	0.34	<0.01	0.02	0.17	<0.01	0.90	0.46					
DEL-WS12-UU														
DEL-WS12-AF	22.25	0.03	<0.01	<0.01	<0.01	0.05	<0.01	0.10	0.54					
DEL-WD12-UU														
DEL-WD12-AF	4.98	0.02	<0.01	<0.01	0.02	0.01	<0.01	0.27	1.69					
DEL-WS13-UU														
DEL-WS13-AF	18.90	0.02	<0.01	<0.01	0.01	0.04	<0.01	0.38	0.25					
DEL-WS14-UU														
DEL-WS14-AF	22.20	0.06	0.29	<0.01	0.04	0.12	0.01	1.30	0.45	4.04	<0.01	0.40	0.30	
DEL-WS15-UU	20.61	0.02	<0.01	<0.01	<0.01	<0.01	<0.01	0.14	1.30					
DEL-WS15-AF	20.28	0.02	<0.01	<0.01	0.03	<0.01	<0.01	0.11	1.33					
DEL-WS16-UU	9.06	<0.01	<0.01	<0.01	<0.01	<0.01	<0.01	0.12	0.50					
DEL-WS16-UU/F	1.41	<0.01	<0.01	<0.01	<0.01	0.01	<0.01	0.01	0.43					
DEL-WS17-UU	13.15	0.01	1.00	<0.01	0.04	0.13	0.01	6.39	0.31					
DEL-WS17-AF	12.28	0.05	0.54	<0.01	0.05	0.11	0.01	5.49	0.30					
DEL-WS22-UU	1.56	<0.01	<0.01	<0.01	<0.01	0.02	<0.01	0.17	3.00					DEL-WS2-UU (BOD Sample):
DEL-WS22-UU/F	0.56	<0.01	<0.01	<0.01	<0.01	0.02	<0.01	0.17	1.69					
DEL-WS25-UU	0.90	<0.01	0.10	<0.01	<0.01	0.01	<0.01	0.23	2.62					Harbour Water near DEL-WS2:

Table 3 (continued) Groundwater and surface-water chemistry – analytical results

Sample Number	Na (mg/l)	K (mg/l)	Ca (mg/l)	Mg (mg/l)	Cl (mg/l)	Sulphate (mg/l)	P (mg/l)	Nitrate (mg/l)	Bi-carbonate (mg/l)	As (mg/l)	Sn (mg/l)	Mo (mg/l)	Cr (mg/l)	Zn (mg/l)	Cd (mg/l)	Pb (mg/l)	Ba (mg/l)	Co (mg/l)	Fe (mg/l)	B (mg/l)	Si (mg/l)
DEL-WS25-UU/F										<0.01	<0.01	<0.01	<0.01	0.04	<0.01	<0.01	0.32	0.02	1.23	1.42	2.86
DEL-WS29-UU	1670.00	32.90	115.00	476.00	4252.00	2308.00		< 0.01	13	<0.01	0.05	0.03	<0.01	<0.01	<0.01	<0.01	6.90	0.02	1.44	0.69	18.51
DEL-WS29-UU/F										0.03	<0.01	<0.01	0.01	<0.01	<0.01	<0.01	0.04	5.15	0.01	0.02	0.78	14.36
DEL-WS42-UU	151.00	8.40	12.70	32.60	255.00	168.00		0.6	< 1	0.08	<0.01	0.01	<0.01	0.21	<0.01	0.03	0.12	0.04	0.23	0.04	3.45
DEL-WS42-UU/F										<0.01	0.05	<0.01	0.01	0.21	<0.01	0.01	0.19	0.02	0.06	0.03	3.15
DEL-WS45-UU	139.00	6.10	9.60	23.50	231.00	118.00		0.4	< 1	<0.01	<0.01	0.01	<0.01	0.05	<0.01	<0.01	0.16	<0.01	0.39	0.04	1.91
DEL-WS45-UU/F										<0.01	<0.01	<0.01	<0.01	0.05	<0.01	0.01	0.14	0.01	0.19	0.04	2.03
R-WS1-UU	8.00	<0.01	72.00	71.50	10.70	3274.00		0.82	< 1	<0.01	<0.01	<0.01	<0.01	0.45	0.04	0.10	0.20	0.71	20.42	0.88	52.88
R-WS1-UU/F										0.06	0.05	<0.01	<0.01	0.46	0.02	0.05	0.15	0.59	16.40	0.76	53.23
R-WD1-UU								0.42	< 1	0.11	0.02	<0.01	<0.01	0.20	<0.01	<0.01	0.22	0.04	17.13	0.26	46.03
R-WD1-AF	9.19	<0.01	38.39	44.76	84.66	3307.75				0.00	<0.01	<0.01	<0.01	0.21	0.03	0.02	0.32	<0.01	16.72	0.66	44.77
R-WS2-UU								5.01	< 1												
R-WS2-AF	8.85	2.64	34.58	37.12	5.08	2000.34				0.24	<0.01	<0.01	0.01	0.75	<0.01	<0.01	0.51	0.26	13.96	0.02	75.74
R-W2D-UU								2.42	< 1	<0.01	<0.01	<0.01	<0.01	0.38	<0.01	<0.01	0.32	0.14	1.81	<0.01	55.03
R-W2D-AF	9.19	1.31	21.21	21.11	145.45	1124.24				0.22	<0.01	<0.01	<0.01	0.42	<0.01	<0.01	0.58	0.13	14.59	0.02	53.06
R-W3-UU								1	< 1												
R-W3-AF	6.18	1.72	20.25	14.78	28.35	747.34				<0.01	0.02	<0.01	<0.01	0.36	<0.01	<0.01	0.96	0.13	5.43	0.04	47.27
H-W1-UU								< 0.01	< 1	0.19	<0.01	<0.01	0.01	1.20	<0.01	0.04	0.20	0.48	14.19	<0.01	78.17
H-W1-AF	1.67	<0.01	54.44	67.33	62.22	2927.78				0.02	<0.01	<0.01	<0.01	1.12	<0.01	0.04	0.36	0.40	19.26	0.16	86.95
H-WS2-UU								0.24	< 1												
H-WS2-AF	7.37	<0.01	21.21	23.03	<0.01	1179.80				0.04	0.04	<0.01	<0.01	0.14	<0.01	<0.01	1.11	<0.01	17.37	0.25	55.42
H-WD2-UU								< 0.01	< 1												
H-WD2-AF	3.13	<0.01	33.33	37.88	29.29	2909.09				0.23	<0.01	<0.01	<0.01	0.07	0.03	0.01	0.33	<0.01	16.67	0.59	52.07
H-W3-UU	4.60	2.00	34.00	50.80	29.50	2362.00		0.32	< 1	<0.01	<0.01	<0.01	<0.01	0.52	<0.01	0.03	0.47	0.01	21.48	0.18	23.62
H-W3-UU/F										<0.01	0.07	<0.01	<0.01	0.56	<0.01	0.01	0.19	0.05	17.25	0.17	23.5
N-W1-UU	5.40	<0.01	25.00	15.00	14.30	448.00		< 0.01	< 1	0.04	0.06	<0.01	<0.01	1.26	<0.01	0.03	0.39	0.16	16.14	<0.01	59.92
N-W1-UU/F										<0.01	0.04	<0.01	<0.01	0.30	<0.01	0.03	0.32	0.12	14.87	0.02	56.20
N-W2-UU								< 0.01	< 1												
N-W2-AF	8.21	<0.01	20.51	15.49	1.03	1410.26				0.18	<0.01	<0.01	<0.01	0.28	<0.01	<0.01	1.18	<0.01	17.55	0.31	59.23
N-W3-UU								< 0.01	< 1	0.09	<0.01	<0.01	<0.01	0.49	<0.01	0.19	0.25	0.38	11.88	<0.01	77.58
N-W3-AF	13.98	<0.01	14.39	23.57	1.02	1559.18				<0.01	<0.01	<0.01	<0.01	0.23	<0.01	<0.01	0.95	0.13	17.55	0.29	68.73
N-W4-UU	9.50	2.10	14.30	20.00	14.80	675.00		0.31	< 1	<0.01	0.06	<0.01	0.04	0.33	<0.01	<0.01	0.28	0.15	3.71	<0.01	86.20
N-W4-UU/F										<0.01	0.08	<0.01	<0.01	0.34	<0.01	0.02	0.24	0.17	3.63	<0.01	75.32
D-W1-UU								< 0.01	< 1	0.03	<0.01	<0.01	0.01	0.48	<0.01	0.18	0.22	0.32	11.72	<0.01	35.31
D-W1-AF	29.67	1.00	42.22	33.44	48.89	1985.56				0.33	0.07	<0.01	<0.01	0.48	<0.01	0.08	0.54	0.28	16.80	0.03	36.31
D-W2-UU								< 0.01	< 1												
D-W2-AF	12.22	<0.01	60.00	26.89	<0.01	3692.22				0.22	0.05	<0.01	<0.01	0.74	0.02	0.01	0.26	0.32	18.67	0.46	67.71
D-W3-UU								0.71	< 1	0.32	0.03	<0.01	0.01	0.93	<0.01	0.19	0.23	0.60	17.97	0.04	63.64
D-W3-AF	0.56	1.56	52.22	31.89	1.11	3194.44				0.00	<0.01	<0.01	0.02	0.94	<0.01	0.13	0.40	0.60	19.47	0.06	62.07

Table 3 (continued) Groundwater and surface-water chemistry – analytical results

Sample Number	Mn (mg/l)	V (mg/l)	Cu (mg/l)	Ag (mg/l)	La (mg/l)	Ni (mg/l)	Y (mg/l)	Al (mg/l)	Sr (mg/l)	Se (µg/l)	Sb (µg/l)	Tl (µg/l)	Hg (µg/l)	Comments
DEL-WS25-UU/F	0.95	<0.01	0.07	<0.01	<0.01	0.02	<0.01	0.23	2.62					
DEL-WS29-UU	4.60	<0.01	<0.01	<0.01	<0.01	<0.01	<0.01	0.08	1.20					DEL-WS1-UU (SOD Sample):
DEL-WS29-UU/F	3.65	<0.01	<0.01	<0.01	0.01	<0.01	<0.01	0.08	0.19					
DEL-WS42-UU	2.15	<0.01	1.30	<0.01	<0.01	<0.01	<0.01	3.18	0.11					Harbour Water near DEL-WS12:
DEL-WS42-UU/F	2.00	<0.01	1.30	<0.01	<0.01	0.01	<0.01	3.18	0.11					
DEL-WS45-UU	0.47	<0.01	0.26	<0.01	<0.01	0.04	<0.01	0.40	0.10					Harbour Water near DEL-WS15:
DEL-WS45-UU/F	0.46	<0.01	0.26	<0.01	0.01	0.06	<0.01	0.39	0.10					
R-WS1-UU	6.36	0.06	1.12	<0.01	0.02	0.18	0.02	12.96	0.18					
R-WS1-UU/F	6.61	0.02	1.22	<0.01	0.04	0.19	0.02	12.96	0.18					
R-WD1-UU	5.20	0.01	0.30	<0.01	<0.01	0.22	<0.01	3.83	0.10					
R-WD1-AF	4.98	0.03	0.01	<0.01	0.03	0.22	<0.01	3.18	0.10	<0.01	<0.01	0.30	0.61	
R-WS2-UU														
R-WS2-AF	4.75	<0.01	3.81	<0.01	<0.01	0.88	<0.01	22.93	0.12					
R-W2D-UU	2.32	<0.01	2.02	<0.01	<0.01	1.13	<0.01	12.98	0.08					
R-W2D-AF	2.26	<0.01	1.89	<0.01	<0.01	1.03	<0.01	12.22	0.08					
R-W3-UU														
R-W3-AF	0.91	<0.01	1.01	<0.01	<0.01	0.19	<0.01	11.97	0.07					
H-W1-UU	14.28	<0.01	6.22	<0.01	<0.01	0.15	0.01	15.38	0.25					
H-W1-AF	13.86	<0.01	5.44	<0.01	<0.01	0.16	<0.01	11.82	0.24					
H-WS2-UU														
H-WS2-AF	5.85	<0.01	<0.01	<0.01	<0.01	0.04	<0.01	0.05	0.07	0.71	2.02	0.10	<0.01	
H-WD2-UU														
H-WD2-AF	12.29	0.01	<0.01	<0.01	0.02	0.02	<0.01	1.66	0.10					
H-W3-UU	12.52	<0.01	1.67	<0.01	<0.01	0.38	<0.01	4.88	0.13					
H-W3-UU/F	12.76	<0.01	1.67	<0.01	0.01	0.42	0.01	4.88	0.14					
N-W1-UU	2.67	<0.01	3.20	<0.01	<0.01	0.07	<0.01	3.21	0.07					
N-W1-UU/F	2.59	<0.01	1.01	<0.01	0.01	0.08	<0.01	1.67	0.06					
N-W2-UU														
N-W2-AF	1.29	<0.01	0.02	<0.01	<0.01	0.03	<0.01	0.81	0.06					
N-W3-UU	0.87	<0.01	4.34	<0.01	0.01	0.22	0.01	26.50	0.09					
N-W3-AF	0.86	<0.01	<0.01	<0.01	<0.01	0.18	<0.01	10.38	0.09					
N-W4-UU	0.50	<0.01	2.50	<0.01	<0.01	0.08	<0.01	13.00	0.05					
N-W4-UU/F	0.52	<0.01	2.50	<0.01	0.01	0.11	<0.01	13.08	0.05					
D-W1-UU	7.71	<0.01	2.69	<0.01	<0.01	0.07	0.01	14.15	0.13					
D-W1-AF	7.49	<0.01	2.56	<0.01	<0.01	0.08	<0.01	13.85	0.15					
D-W2-UU														
D-W2-AF	4.87	0.01	6.56	<0.01	0.01	0.08	0.02	15.44	0.16					
D-W3-UU	8.29	<0.01	9.84	<0.01	0.01	0.08	0.02	25.52	0.15					
D-W3-AF	8.24	<0.01	9.65	<0.01	0.02	0.07	0.02	24.64	0.15	<0.01	<0.01	<0.01	10.44	

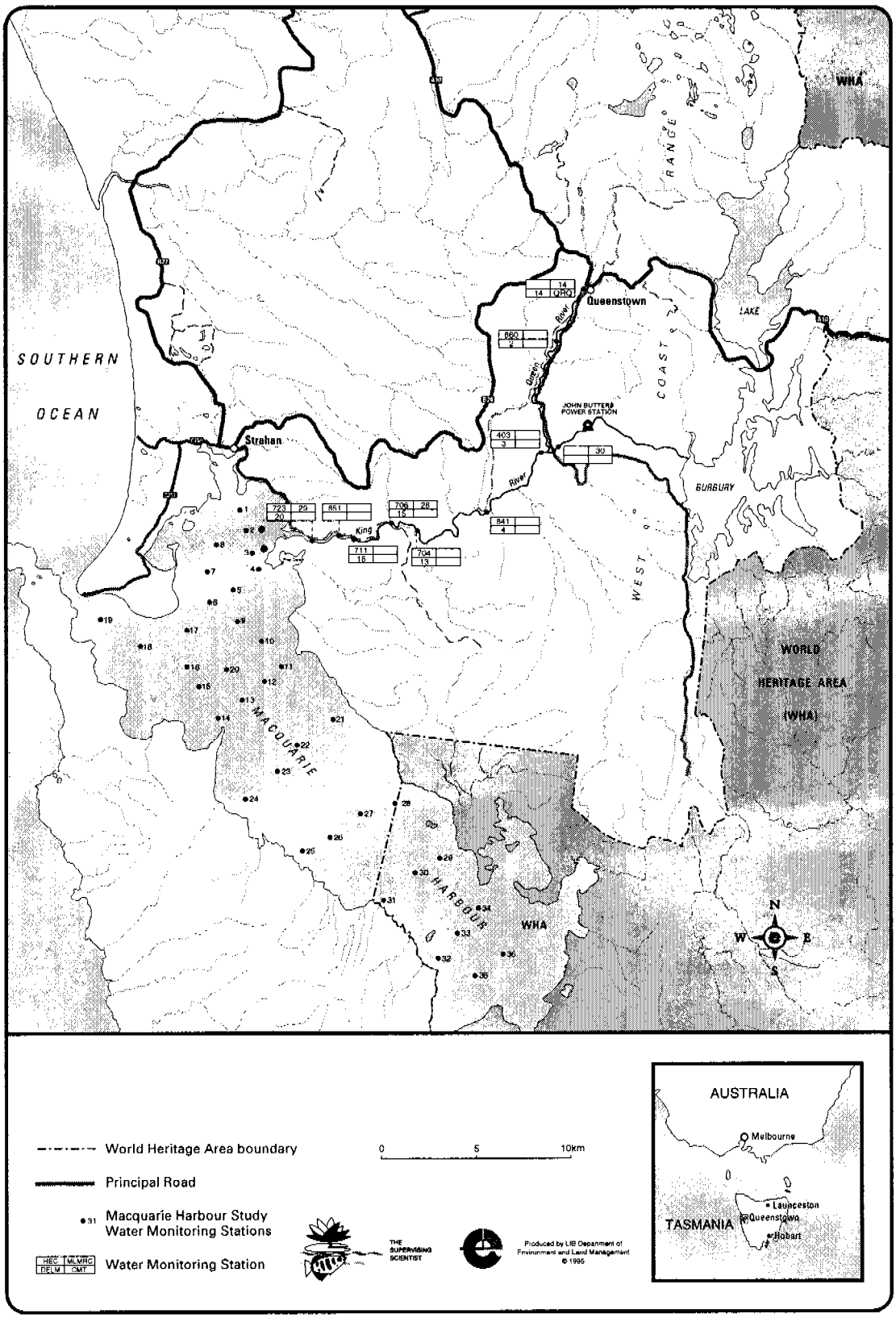

Figure 23 Location of regional water monitoring stations

appears to be largely soluble in groundwater samples, and displays elevated concentrations in acidic portions of the north lobe (0.04 to 0.13 mg/L). Lead is largely in soluble form in groundwater samples, and ranges from BDL up to 0.19 mg/L. Elevated Pb concentrations are rare and are largely confined to the north lobe in the more acidic samples. High Co concentrations in largely soluble form are found in most of the acidic groundwater in the delta, and range from BDL to ≈2.0 mg/L.

Selenium, Hg, Sb and Tl analyses were only conducted on seven groundwater samples. As predicted by EGI (1991c), Se concentrations are relatively high for some samples (eg DEL-WS2: 106 µg/L). Although the limited results were highly variable, the distribution of Se suggests that elevated aqueous concentrations may be favoured by reducing and near-neutral conditions. ANZECC guidelines for the protection of aquatic ecosystems provide a recommended criteria for total Se in fresh water of 1 to 10µg/L. Concentration ranges for Hg were also variable, with a single high of 9.4 µg/L in groundwater within Bank D. Concentrations of Sb and Tl were uniformly low, with values ranging from BDL to 2.0 µg/L, and BDL to 3.3 µg/L respectively. Aqueous Ag concentrations are BDL for all groundwater samples.

Detectable bicarbonate concentrations were recorded in four reduced groundwater samples from the delta in the tidal interface zone (1 to 87 mg/L). These values are believed to reflect the influence of microbial activity, but are likely to have been significantly lowered by exsolution of CO_2 during transport to the laboratory. Loss of H_2S gas is also likely to have lowered total sulphur concentrations in samples where a strong odour was detected (ie DEL-WS12, DEL-WD12, N-W3 and H-WD2).

Nitrate was detected in groundwater samples on both the banks and delta. Concentrations are generally low and range from BDL to 23.6 mg/L. The unpredictable pattern of nitrate concentrations suggests that it is strongly influenced by the haphazard distribution of organic debris. Harbour water samples (DEL-WS25, DEL-WS45 and DEL-WS42) contained between 0.4 to 565 mg/L nitrate, indicating that some nutrients could be supplied to groundwater in the delta by brackish harbour water. Ammonia and nitrite were not analysed, but should be included in future work, especially for highly reduced groundwater samples (eg the tidal zone on delta). All of the groundwater samples from piezometers on the north lobe of the delta were analysed for phosphorous, to identify potential limiting factors for the growth of bacterial populations. Analysis was conducted on filtered/acidified samples, and a single on-scale reading of 0.2 mg/L was obtained in sample DEL-WD1. This is regarded as relatively high for soluble phosphorous, and being in the tidal zone may reflect contributions from the harbour water.

Chloride concentrations range from BDL to 4380 mg/L, and are significantly elevated in the delta groundwater. Na, Ca, Mg and SO_4 are similarly elevated in delta groundwater samples relative to sediment bank deposits, indicating the likely interaction of sea water and groundwater in the delta. This is predicted to be the result of periodic inundation of the delta by brackish harbour water. This process appears to be responsible for significant differences in the chemistry of the delta groundwater relative to the sediment bank deposits. For example, periodic inundation is likely to be responsible for a net increase in sulphate, chloride and nutrients in groundwater in the delta. Despite this chemical signature of periodic inundation of the delta, K is conspicuously low in all but the three most reduced (ie sulphate poor) delta groundwater samples. This suggests that K is being removed by mineral saturation reactions (eg jarosite).

In the delta, reduced near-neutral groundwater samples associated with organic-rich material and bacterial activity generally display the lowest aqueous metal and acid concentrations, although Fe, Si, Mn and As remain elevated. This observation highlights the importance of naturally occurring bioremediation as a crucial process in controlling water quality.

The chemistry of groundwater in the banks and delta is highly variable, and appears to be at least partly controlled by local differences in tailings composition, particularly the organic and clay content. Data for pH, EC and Eh were recorded for the water table (upper 10 cm of groundwater) along selected traverses on the delta (figures 19, 20 and 21, tables 3 and 4). Groundwater varies from highly oxidised (530 mV) and acidic (pH 2.54) to near neutral (pH 7.10) and relatively highly reduced (-57 mV). Field conductivity measurements also revealed low (400 µS/cm) to very high electrical values (≈30 000 µS/cm), with the higher conductivities reflecting interaction of brackish harbour water with the delta sediments (eg DEL-WS1, DEL-WD1, DEL-WS2, DEL-WS3 and DEL-WS15). No consistent variation in groundwater chemistry was noted with distance from the harbour water, in either pH, EC or Eh. Significant increases in the EC of groundwater at the water table were noted to be empirically related to the local abundance of clay material, possibly indicating enhanced cation exchange.

The chemistry of groundwater in the south lobe of the delta is less variable and more acid than in the north lobe, probably reflecting a lower organic content and less microbial activity in the former. These results clearly indicate that pore water in the delta is not always near neutral, as suggested by EGI (1991c). Furthermore, this study has demonstrated that despite a paucity of sulphides in the upper 10 cm of the delta tailings, there is significant acid forming capacity in these sediments.

Acid generation

Groundwater at the water table in the delta displayed distinct differences from deeper groundwater as measured from nearby piezometers (figures 19, 20 and 21, table 4). The upper layer of groundwater is generally highly acid, with the magnitude of pH increases with depth being dependent on local tailings composition. Increases of 2 to 3 pH units were recorded from the water table to deep (1 to 1.5 m) groundwater in the north lobe of the delta (eg DEL-WS8: 3.93 to 6.5 over 120 cm). The groundwater at the water table in the north lobe also displays significantly lower conductivity than deeper groundwater from piezometers. Increases in EC in the order of 2 to 5 times are recorded with depth (eg DEL-WS8; 700 to 3800 µS/cm over 120 cm). These changes are also associated with progressively reducing conditions with depth (eg DEL-WS8: 256 to -2 mV over 120 cm). Similar trends in pH and Eh are also evident in the south lobe, but no field EC readings were taken from groundwater from the piezometers.

Chemical differences between the water table and deeper groundwater suggests that acid production in the upper layer of groundwater in the delta may be controlled by processes other than direct sulphide oxidation. Similar conclusions can be drawn from data in EGI (1991c) on the chemistry of groundwater from the delta. Their results indicate that in the laboratory the pH of pore water becomes slightly more acid over time, while the EC decreases significantly. In addition, it is evident from the study by EGI (1991c) that surface layers in the delta contain more acid-generating material than less oxidised deeper material, and that the relatively rapid decrease in the pH of extract water (not in contact with sediment) over 2 days suggests that some reduced aqueous iron and/or sulphur species are highly reactive.

Despite an apparent paucity of pyrite, there is abundant acid forming material in the upper few centimetres of the tailings material in both the delta and the river banks. Rainwater accumulating in puddles on the surface of the delta exhibits within seconds to minutes pH values in the range of 2.9 to 3.5. Surface and near-surface runoff from the tailings banks behaves similarly. This acidity is probably enhanced by periodic dissolution of acid forming material by rainwater, and subsequent evaporation in disconnected pools on both banks and delta. When the pools combine to form runoff during heavy and persistent rainfall, short-term acid contributions to the river and harbour are significant.

The migration of groundwater containing acid forming material in the form of reduced aqueous species, and its subsequent near-surface oxidation is consistent with chemical gradients observed in groundwater, and the latent acidity of surficial tailings during rainfall events (see Discussion – Acid production).

Sediment mineralogy and mineral chemistry

General

Sedimentary deposits in the King River and its delta are comprised of pre-mine siliceous detritus and overlying siliceous and sulphidic tailings residue from the copper concentration process at the Mount Lyell mine. Both the sediment banks and delta are dominated by tailings material. Pre-mine and tailings sediment in the overbank deposits, and the upper 1 to 4 m of the delta are coated with a thin veneer of orange iron oxyhydroxide.

Pre-mine sediments

Petrographic data on original sedimentary material were compiled from the samples R-C1-730-745, R-C1-580-600 and DEL-C1-420-550. Pre-mine sediments are comprised of subangular to subrounded silt and fine to coarse-grained sandy detritus containing silicic volcanics (25 vol%), vein quartz (25 vol%), microcrystalline silica (15 vol%), meta-sedimentary rock fragments (25 vol%), assorted accessory crystal components (3 to 7 vol%) and miscellaneous organic debris (1 to 5 vol%). Volcanic detritus is almost exclusively silicic, and can include partially resorbed, euhedral quartz phenocrysts, patches of microcrystalline silica, and subordinate muscovite. Vein quartz fragments display crack-seal, space-filling and mosaic textures, and are generally barren. Microcrystalline quartz fragments probably represent volcanic debris, but a metasedimentary origin is also possible. Deformed metasedimentary material such as sericite-chlorite±quartz±epidote schists, siltstones, sandstones and quartzites are present. Accessory crystal components include fine to coarse grained clinopyroxene (trace to 5 vol%), variably weathered K-feldspar and/or plagioclase (trace to 2 vol%), fine to medium grained anhedral magnetite (trace to 1 vol%), fine to coarse grained ilmenite (trace to 1 vol%), subhedral to anhedral fine grained zircon (trace to 1 vol%), and traces of variably retrogressed hornblende, chromite and spinel. Fragments of carbonate and primary sulphides were conspicuously absent from these samples, but rare biogenic pyrite framboids and rims of biogenic pyrite on iron- and/or carbon-rich grains were found in the sample DEL-C1-420-550. This sample indicates that there is a mass transfer of metals from the tailings downward into earlier sediments, and that caution should be exercised when using chemical parameters such as bulk Cu or S concentrations to clarify sedimentary origin.

Mine tailings

The tailings sediment comprises rock and vein fragments from highly altered and mineralised sections of the Cambrian Mount Read Volcanics. At Mount Lyell the volcanics are dominated by felsic to mafic lavas, breccias, lapilli tuffs and volcaniclastics, and the

Table 4 Groundwater and surface-water chemistry – field and laboratory parameters

Sample Number	Sample Volume (cm3)	Analytical Procedures	Volume of 1M HNO3 (cm3)	Field pH Value	Laboratory pH Value	Field Conductivity (µs/cm)	Laboratory Conductivity (µs/cm)	Field Eh (mV)	Field Cu (mg/l)	Dissolved Oxygen (mg/l)	Comments
DEL-WS1-UU	250	1,3	0	6.72	6.4	10100	12970	-0.044			
DEL-WS1-AF	250	2,3	2.5								
DEL-WD1-UU	250	1	0	6.76	6.0	10700	13700	-0.042			
DEL-WD1-AF	250	2,3	2.5								
DEL-WS2- UU	250	1,3	0	7.1	7.3	> 20000	29900	-0.057	0		
DEL-WS2-AF	250	2,3,4,5.	2.5								
DEL-WS3- UU	250	1	0	6.45	4.3	9300	11610	-0.012			
DEL-WS3-AF	250	2,3	2.5								
DEL-WS4- UU	250	1	0	6.53	4.5	5700	7160	-0.024	0.01		
DEL-WS4-AF	250	2,3	2.5								
DEL-WS5- UU	250	1	0	6.48	3.6	2300	2450	-0.037			
DEL-WS5-AF	250	2,3	2.5								
DEL-WS6- UU	250	1	0	6.64	4.2	4300	4740	-0.018			
DEL-WS6-AF	250	2,3	2.5								
DEL-WS7- UU	250	1	0	6.81	4.1	3300	3450	-0.017			
DEL-WS7-AF	250	2,3	2.5								
DEL-WS8- UU	250	1,3	0	6.5	4.3	3800	3800	-0.002	0		
DEL-WS8-AF	250	2,3,4,5.	2.5								
DEL-WS9- UU	250	1,3	0	5.27	4.3		810	0.165			
DEL-WS9-AF	250	2,3,4,5.	2.5								
DEL-WS10-UU	250	1	0	3.94	4.1		1175	0.34			
DEL-WS10-AF	250	2,3	2.5								
DEL-WS11-UU	250	1	0		2.4		1910				
DEL-WS11-UU/F	250	6	0								
DEL-WS12-UU	250	1	0	5.55	4.2		5190	0.132			H2S gas
DEL-WS12-AF	250	2,3	2.5								
DEL-WD12-UU	250	1	0	6.32	5.8		6220	0.008			H2S gas
DEL-WD12-AF	250	2,3	2.5								
DEL-WS13-UU	250	1	0	5.81	3.2		2150	0.043			
DEL-WS13-AF	250	2,3	2.5								
DEL-WS14-UU	250	1	0	5.4	3.3		3070	0.168			
DEL-WS14-AF	250	2,3,4,5.	2.5								
DEL-WS15-UU	250	1,3	0	6.45	5.0		10330	0.044			
DEL-WS15-AF	250	2,3	2.5								
DEL-WS16-UU	250	1	0		7.7		2670				
DEL-WS16-UU/F	250	6	0								
DEL-WS17-UU	250	1,3	0	4.66	3.1		1590	0.2			
DEL-WS17-AF	250	2,3	2.5								
DEL-WS22-UU	700	1	0	7.1	7.8	> 20000	28700	-0.057			
DEL-WS22-UU/F		6									
DEL-WS25-UU	250	1	0	6.62	3.1	16700	22300	0.037			
DEL-WS25-UU/F		6									
DEL-WS29-UU	700	1	0	6.72	6.8	10100	12060	-0.044			
DEL-WS29-UU/F		6									
DEL-WS42-UU	250	1	0	3.84	4.0		1090	0.432			

Table 4 (continued) Groundwater and surface-water chemistry – field and laboratory parameters

Sample Number	Sample Volume (cm3)	Analytical Procedures	Volume of 1M HNO3 (cm3)	Field pH Value	Laboratory pH Value	Field Conductivity (µs/cm)	Laboratory Conductivity (µs/cm)	Field Eh (mV)	Field Cu (mg/l)	Dissolved Oxygen (mg/l)	Comments
DEL-WS42-UU/F		6									
DEL-WS45-UU	250	1	0	4.57	4.4		852	0.304			
DEL-WS45-UU/F		6									
R-WS1-UU	150	1	0	3.65	2.9	1884	2340	0.264			
R-WS1-UU/F		6									
R-WD1-UU	250	1,3	0	4.68	2.4	961	1460	0.19		3	
R-WD1-AF	245	2,3,4,5.	2.5								
R-WS2-UU	250	1	0	3.18	3.0	605	825	0.372			
R-WS2-AF	150	2,3	2.5								
R-W2D-UU	250	1,3	0	3.75	3.3	363	524	0.333			
R-W2D-AF	250	2,3	2.5								
R-W3-UU	250	1	0	3.58	3.5	314	415	0.335			
R-W3-AF	200	2,3	2.5								
H-W1-UU	250	1,3	0	2.99	3.0	1070	1500	0.359			
H-W1-AF	250	2,3	25								
H-WS2-UU	250	1	0	5.74	3.2	530	554	0.056			
H-WS2-AF	250	2,3,4,5.	2.5								
H-WD2-UU	250	1	0	4.43	3.1	960	1560	0.119			H2S gas
H-WD2-AF	250	2,3	2.5								
H-W3-UU	80	1	0	4.38	3.0	1030	1740	0.146			
H-W3-UU/F		6									
N-W1-UU	250	1	0	5.93	3.1	464	895	0.045	0.12	2	
N-W1-UU/F	250	6	0								
N-W2-UU	250	1	0	4.66	3.1	475	872	0.171			
N-W2-AF	40	2,3	1								
N-W3-UU	250	1,3	0	3.9	3.2	526	900	0.144	0.32		H2S gas
N-W3-AF	100	2,3	2								
N-W4-UU	250	1	0	2.72	3.1	652	962	0.522	0.04		
N-W4-UU/F	250	6	0								
D-W1-UU	250	1,3	0	2.72	3.3	1220	1250	0.5			
D-W1-AF	250	2,3	25								
D-W2-UU	250	1	0	2.98	3.1	1290	1600	0.391			
D-W2-AF	250	2,3	25								
D-W3-UU	250	1,3	0	2.54	3.1	1730	1880	0.53			
D-W3-AF	250	2,3,4,5.	25								

Analytical Procedures

1 pH, Eh, T°C, EC, NO3-, HCO3-
2 Na, K, Ca, Mg, Cl-, SO42-,
3 As, Sn, Mo, Cr, Zn, Cd, Pb, Be, Co, Fe, B, SiO2, Mn, V, Cu, Ag, La, Ni, Y, Al, Sr.
4 As, Se, Sb, Tl
5 Hg
6 Filter through 0.45µm and then Na, K, Ca, Mg, Cl-, SO42-, As, Sn, Mo, Cr, Zn, Cd, Pb, Be, Co, Fe, B, SiO2, Mn, V, Cu, Ag, La, Ni, Y, Al, Sr.

overlying sequence includes siltstone and conglomerate (Solomon 1989). Much of the copper mineralisation is syngenetic in origin, and developed by exhalative hydrothermal processes on or near a Cambrian seafloor. Secondary assemblages developed during ore formation include quartz, chlorite, sericite, carbonate and sulphides. The deposits have been subjected to multiple phases of deformation and upper greenschist facies regional metamorphism (Solomon 1989). Metamorphic assemblages include biotite, chlorite, K-feldspar, epidote, albite, sphene and carbonate.

The grain size of tailings disposed to the East Queen River over the life of the mine ranges from <1 μm to ≈1000 μm, with median values ranging from 10 to 80 μm (Locher 1995).

Tailings

Tailings sediments comprise fragments of ore gangue, vein quartz, felsic volcanics, metasedimentary material and slag, and assorted crystal components in highly variable proportions. The following relative abundances in detrital components were determined from the petrographic study:

Detrital components	**Vol%**
Rock fragments	
Gangue	40–80
Felsic volcanics	0–10
Metasedimentary	1–10
Vein quartz	1–15
Slag	0–60
Crystal components	
Pyrite (FeS_2)	0–10
Chlorite $(Fe,Mg)_5Al_2Si_3O_{10}(OH)_8$	0–3
Muscovite $(KAl_3Si_3O_{10}(OH,F)_2$	0–3
Carbonate ($MeCO_3$)	0–5
Magnetite (Fe_3O_4)	0–3
Ilmenite ($FeTiO_3$)	0–1
Chromite ($FeCr_2O_4$)	0–trace
Zircon ($ZrSiO_4$)	0–trace
Organic matter	1–5

Fragments of ore gangue are quartz-rich rocks containing varying proportions of fine to coarse grained foliated to decussate aggregates of chlorite (chamosite; Appendixes 3 and 4, analyses A4.43 to A4.48) and white mica (muscovite-2M; Appendix 3), as well as euhedral to subhedral pyrite±chalcopyrite crystals (plate 13). Other sulphides including sphalerite, galena and bornite are also observed occasionally in these fragments. Fine to coarse grained, euhedral to subhedral carbonate crystals (often Mn-rich siderite; Appendix 4, analyses A4.34 to A4.42) are occasionally distributed throughout the gangue fragments. In some situations, sulphides and carbonates are completely encased by a silicate matrix, and in other cases are exposed to fluid interaction along fragment boundaries. Some of the gangue fragments are coarse grained aggregates or crystals of chlorite, with lesser chlorite+muscovite or muscovite alone.

Other rock fragments include mica-schists and quartz-mica schists, and these either represent foliated gangue or metasedimentary material. Sandstone and siltstone detritus is relatively rare. Schistose rocks include chlorite, chlorite+sericite, and muscovite+quartz ±chlorite varieties, and can include accessory phases such as carbonate, biotite, magnetite, rutile,

ilmenite, zircon, sphene, epidote and pyrite. Altered silicic volcanic fragments are dominated by microcrystalline quartz, with minor retrogressed feldspar phenocrysts and varying proportions of sericite. Quartz vein fragments displaying fibrous crack-seal, irregular mosaic, granoblastic and open-space growth textures are common. Accessory sulphide components within the vein material are rare, but can include pyrite±chalcopyrite.

Slag represents slightly in excess of 1% of the total volume of mine waste disposed of to the Queen River, and appears to be almost exclusively restricted to the river bottom and upper delta deposits. In the upper sections of the river bottom sediment pile, the slag comprises at least 40 to 50 vol%, but probably averages from 1 to 3 vol% in the upper 1 to 2 m of the delta. The slag is a grey-brown-black, subrounded to subangular glassy product derived from the smelting of copper ore. Microprobe analyses of anhydrous slag indicate that it is largely a Fe-Cu sulphide saturated iron-silicate glass, containing lesser proportions of Al, Mg and K (Appendix 4, analyses A4.1 to A4.7). Chemical data in table 5 highlight the iron-rich nature of the slag, and clearly demonstrate that it is also relatively enriched in Zn, Cu, Co, Pb, Mo and Cr (see Leach tests). Fracturing to produce characteristically cuspate margins and cuspate shards, the slag generally contains significant proportions (2 to 5 vol%) of rounded, immiscible sulphide-melt inclusions (Fe-Cu-S; plate 14, Appendix 4, analyses A4.16, A4.25 to A4.28,) and rare euhedral crystals with the morphological and optical properties of olivine. Based on the chemistry of the slag, this phase is probably fayalite (Fe_2SiO_4). The anhydrous slag composition (Appendix 4, analyses A4.1 to A4.7) provides a general indication of the bulk chemistry of fresh tailings material.

Post-depositional modification of the slag is widespread, particularly in samples that are at least partially subaerial, and can be intense in places (see description of KR-1 below). Alteration commences with hydration of the outer layers of the slag. Microprobe data indicate that this involves a major depletion of iron. This is supported by the development of intense red staining on the inside of plastic bottles containing water-saturated slag-rich samples, and the formation of 'hardpan' layers (see below). Modification proceeds by the development of concentric zones of hydration layers, which often mimic the initially cuspate borders of the slag fragments. When Cu-Fe-sulphide melt blebs are encountered during slag hydration, the alteration front progresses around the sulphides, leaving unaltered blebs surrounded by concentric hydrated layers (plate 14). Some time later, the sulphides succumb to oxidation and disappear (plate 14). Plate 19 (see p.71) displays a cross section through the finely layered hydrated shell of a slag fragment. Microprobe data indicate that slag hydration and Fe depletion are accompanied by losses of Ca, Mg and K, and relative increases in Si, Al, S, Ti, Cu and Zn (Appendix 4, analyses A4.9 to A4.15, A4.19 to A4.22).

Pyrite varies from coarse grained (50 to 100 μm) angular detritus (plate 13) to ultra-fine grained (<0.1μm) framboidal crystals of biogenic origin forming circular clusters and grain coatings (plate 15). Primary pyrite occurs as both individual crystals and as a common component of gangue rock fragments. Rounded and irregular inclusions of chalcopyrite are not uncommon in pyrite. Chalcopyrite rarely occurs as discrete grains, and is usually associated with gangue-bearing rock fragments, commonly containing quartz+chlorite+ pyrite±muscovite. Subordinate sulphides often intimately associated with chalcopyrite include sphalerite, sometimes galena and rarely bornite. Magnetite is occasionally found adjacent to chalcopyrite.

Large discrete crystal fragments of carbonate are widespread throughout saturated tailings. Limited analytical work indicates a predominance of Mn-rich siderite (Appendix 4, analyses

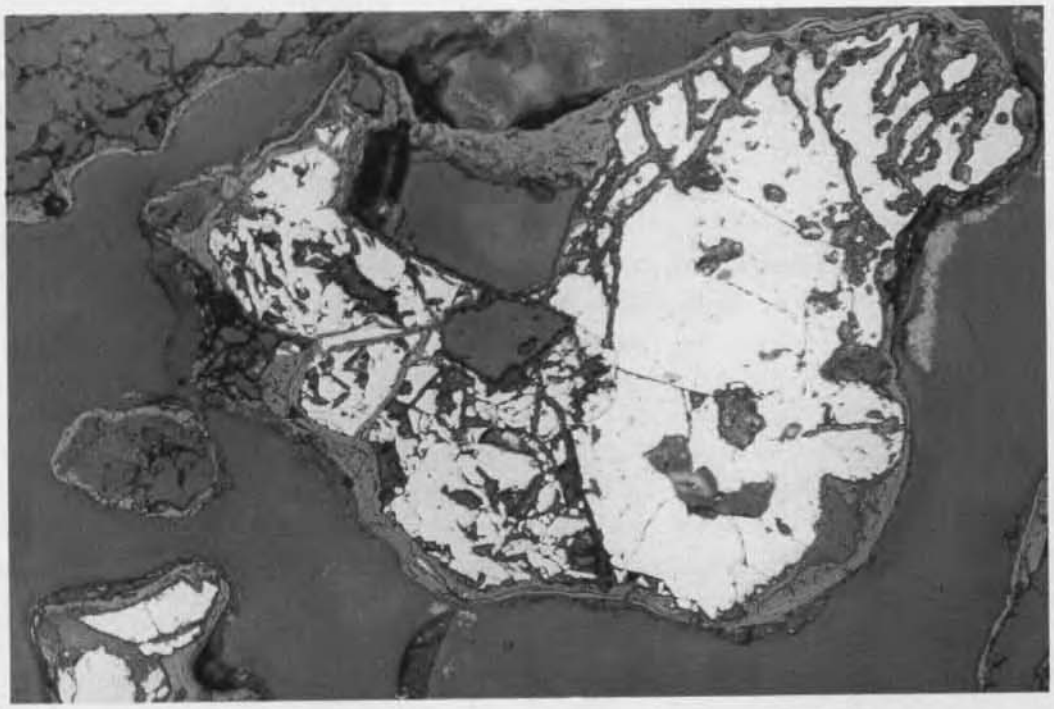

Plate 13 Reflected light photomicrograph of sample DT-1. This sample is from unsaturated, partially cemented outcrop on the south lobe of the delta. A large partially degraded, highly fractured pyrite aggregate (white) is encased by a delicately banded iron-oxide layer (light-grey). The iron-oxide has penetrated most fractures within the pyrite and appears to have assisted its preservation. The horizontal dimension of the plate is ≈450 μm.

Plate 14 Reflected light photomicrograph of sample DT-1. Two silicate grains (left) and a variably hydrated slag fragment (centre-right) are cemented by iron-oxide (?goethite; thinly banded light-grey rims on all grains). Anhydrous slag material (light-grey) is surrounded by partially hydrated slag (medium-grey) and intimately banded, strongly hydrated and altered slag. Much of the slag fragment is highly fractured and contains small, circular Fe-Cu sulphide melt blebs (white spots) or pseudomorphs thereafter. The horizontal dimension of the plate is ≈450 μm.

A4.34 to A4.42). A range of accessory crystal components are observed, sometimes associated with a small proportion of country rock, but generally as discrete crystals. These include magnetite, ilmenite, chromite, zircon, spinel and hematite.

All of the tailings samples examined contained organic debris, ranging from pollen, seeds, leaf litter and wood fragments. The organic content of tailings varies significantly, but is estimated to average ≤1 vol%. SEM work revealed the presence of amorphous carbon material providing a weak binding medium for grains of sediment from water saturated, reduced samples. This substance may be the product of microbial activity on decayed plant matter, and may provide the substrate for biogenic pyrite precipitation (see below).

Although significant chemical degradation of the tailings is occurring, little evidence of these changes is evident in most grains. Signs of alteration and dissolution are scant, presumably due to relatively high rates of fluid flow and rapid dissolution, but there is a clear indication of secondary precipitation. The widespread orange iron-oxide coating is the best evidence of chemical modification. Grains in unsaturated tailings, particularly those in slag-rich samples, generally display thicker iron-oxide coatings than in saturated samples. The distribution of the iron-oxide coatings is a direct reflection of the maximum extent of oxidation of reduced groundwater, and has no direct relationship to the extent of sulphide oxidation. For example, almost 2 m of pre-mine sediments on Bank R are iron stained.

Saturated tailings

Most of the detrital pyrite, and other sulphides, in saturated tailings deposits appears very fresh. Progressive destruction/dissolution of pyrite is generally only evident in the highly reduced, water saturated samples where the dissolution process has been reversed and preserved by biogenic sulphide precipitation. In most saturated samples, oxidation appears to be focussed on the margins of pyrite grains, and groundwater flow rates appear to be too rapid to preserve degraded rims or sulphate by-products.

Small quantities (trace to 1 vol%) of framboidal biogenic pyrite are evident in several of the more reduced, organic-rich, water saturated sediment samples (eg DEL-WS12-S, DEL-WD8-S, DEL-WS3-S, DEL-C1-420-550 and R-C1-250-280). Biogenic pyrite occurs as circular concentrations of framboids, and as thin veneers lining the margins of silicate-bearing rock and sulphide fragments which are initially coated with amorphous organic matter (plate 15). Biogenic pyrite is also observed lining and disseminated throughout organic fragments, eg leaf litter and wood. The organic coating on grains appears to be providing a reduced substrate for sulphide deposition. Rare examples of biogenic chalcopyrite can be seen in the samples DEL-WS12-S and DEL-WS3-S, where delicate botryoidal growth habits are preserved on the margins of silicate grains (plate 16).

Crystal fragments of carbonate minerals were observed in water-saturated samples, but were absent from the water-unsaturated zone. Despite being in contact with relatively acid groundwater, carbonate was still present in many water-saturated samples, but appeared to have undergone complete dissolution in nearby water-unsaturated zones.

Geological logging of river bottom sediments conducted by Locher (1995) indicated an abundance of slag, and this was supported by recent drill samples collected by Locher (MLRRDP project 4, forthcoming publication) and examined in this study (Appendix 1, figure 5). One polished section was prepared from this material from upstream of the Teepookana Bridge (sample KR-1, figure 24). The sample KR-1 represents a 'hardpan' or strongly cemented slag-rich layer that develops on the upper surface of the river bottom sediments. The distribution of this layer as mapped by Locher (1995) is shown in figure 24. The

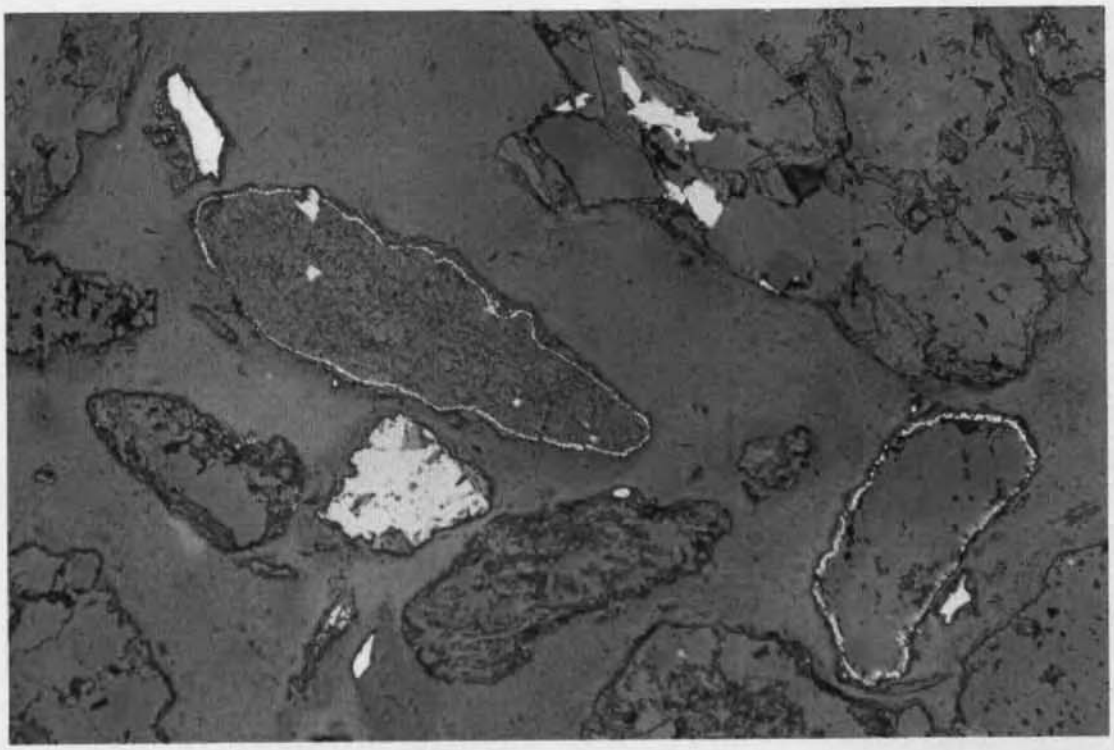

Plate 15 Reflected light photomicrograph of sample DEL-WS3-S. This sample was recovered from adjacent to the sceened zone of piezometer DEL-WS3 on the north lobe of the delta, at a depth of 50 cm. Two silicate rock fragments exhibit continuous rims of biogenic pyrite. Detailed evalution of the grain boundaries reveals that the sulphide is associated with very fine grained (?amorphous) organic material. The horizontal dimension of the plate is ≈450 μm.

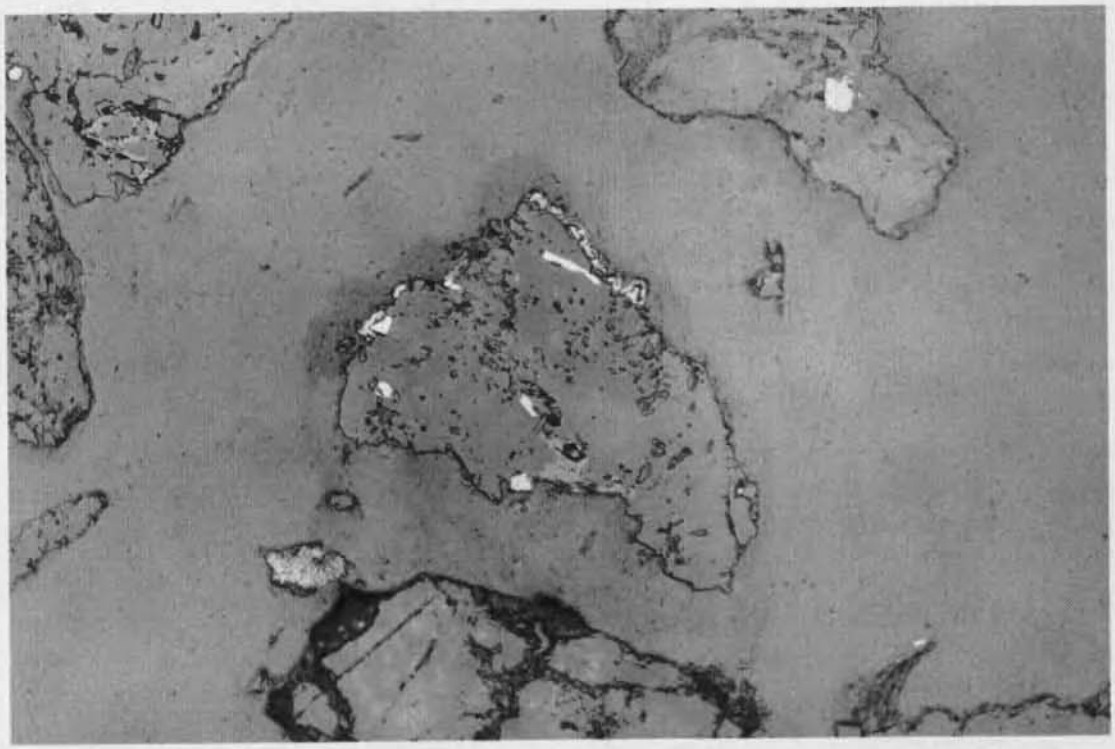

Plate 16 Reflected light photomicrograph of sample DEL-WS3-S. The quartz-rich rock fragment in the centre of the plate is host to a thin rim of biogenic chalcopyrite with a botryoidal habit The horizontal dimension of the plate is ≈450 μm.

KR-1 'hardpan' is comprised of 35 to 40 vol% slag, 40 to 45 vol% siliceous gangue rock fragments, 5 to 10 vol% vein quartz grains, and roughly 5% coarse, fresh pyrite±chalcopyrite grains. Other accessory crystal components (total ≤5%) include siderite (manganese-rich solid solution), magnetite, ilmenite and zircon. Most detritus is coated with a relatively thick layer of iron-oxide. The role of this coating around carbonate grains for inhibiting acid neutralisation is unknown, but may be important.

The cementation process appears to result from the mobilisation of iron from the slag and its precipitation as iron-oxide around grain boundaries (plates 13 and 14). This has been facilitated by the increase in molar volume associated with progressive hydration of slag fragments (plate 14), which dramatically reduces porosity. Additional data on the process accompanying slag hydration were provided by Back Scattered Electron (BSE) and X-ray mapping techniques. X-ray maps across the hydrated rim of three slag grains identified some elemental depletions and enrichments associated with hydration (plates 17 and 18). The delicate banding in the hydrated rim is comprised of zones of silica, iron and copper enrichment with X-ray statistics indicating a strong association between Fe and S in the grain in plate 17, and between Cu and S in the grain in plate 18. More work would be required to determine the specific environmental processes controlling chemical episodes preserved in the rims. However, the distribution of hardpan layers in the King River river-bed, the distribution and degree of slag hydration, the chemical changes accompanying hydration, and the chemical reactions revealed in saturated river bottom samples all suggest that oxidation is the key factor in alteration and partial dissolution of the slag, as well as in the formation of the hardpan. Successive wetting and drying episodes may also play some role, but no clear evidence for such processes is evident in the unbroken concentrically zoned hydration layers surrounding slag fragments, and it is unlikely that the hardpan is ever unsaturated. Sufficient oxygen may be available from turbulent river water during low flow periods to cause oxidation.

Unsaturated tailings

Petrographic work confirmed field observations from panned concentrates that although highly depleted, minor to trace amounts of fresh pyrite and chalcopyrite are often still present in near-surface unsaturated tailings material both in the banks and delta. Relatively thick coatings of iron-oxide are observed around some of these sulphides in unsaturated samples (plate 13). It is not known to what extent these coatings inhibit sulphide dissolution, but results from leach tests suggest that they may be ineffective in this regard (tables 6 and 7, sample DT-1).

Limited chemical data in table 5 indicate a general depletion of Cu and S in the bank sediments relative to the delta, supporting the likelihood of higher rates of leaching from the unsaturated bank deposits.

Secondary phases

XRD analysis of Fe-rich samples (ie DT-1, KR-1) failed to clarify the nature of the iron-oxide precipitate coating most sediment grains. Numerous iron-oxide, iron-sulphate and related hydrates were evaluated, but the only likely assemblage (goethite) consistent with the spectral data has peaks overlapping with other silicate minerals. X-ray spectra from EDS analysis on the IFESEM also indicated that the precipitate was dominated by Fe and O. From these data it may be concluded that the orange precipitate is likely to be predominantly goethite.

All unbroken grains examined by IFESEM were coated with an iron-oxide precipitate, possibly goethite. Though the form and extent of the goethite precipitate varies, the crystal

Figure 24

Surface Characteristics of the King River Bed
(After Locher, 1995)

0 1 2 3km

50m Contour Interval

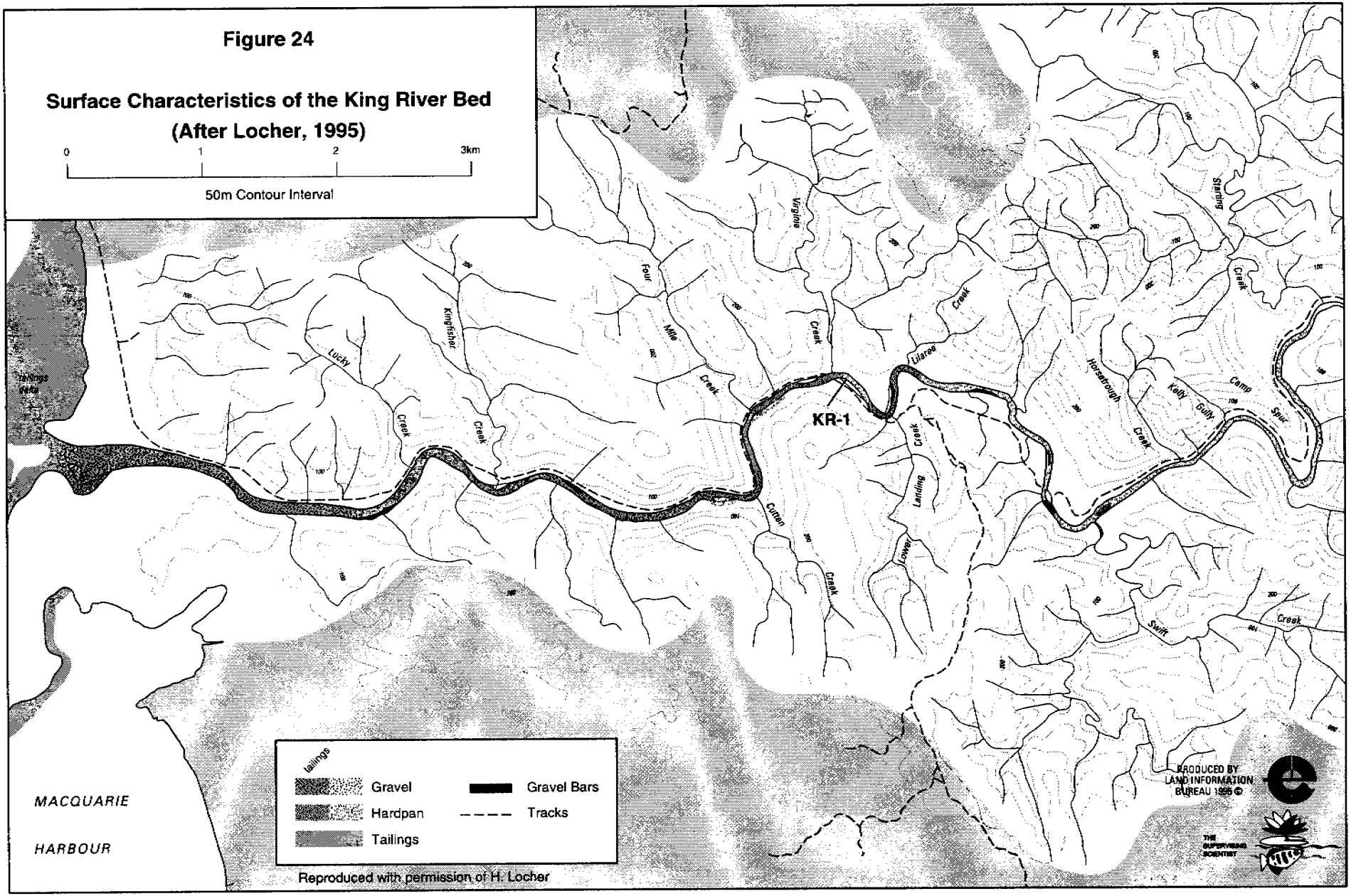

Reproduced with permission of H. Locher

habit is largely as thin bladed aggregates less than 1 μm in length (plates 21 to 28). Almost all X-ray spectra recorded from these iron-oxide surface coatings identified smaller but there were additional persistent peaks for Cu and C (Appendix 5; all spectra). No discrete Cu±Fe±O±C bearing phases were identified visually. The relative proportion of the Fe, O, Cu and C peaks varied significantly, but Cu and C peaks were qualitatively noted to be higher from sediment samples from saturated and reduced settings (eg DEL-WS12-S). Peak counts for Cu and C were observed to accumulate rapidly during the initial seconds of analysis, and taper off during the remaining portion of the 100 second count time. This appeared to indicate that the Cu±Fe±O±C material was a thin surface coating that was largely removed by beam damage early during analysis. Accelerating voltages were lowered to test this hypothesis, and the intensity of Cu and C peaks were qualitatively noted to rise. The Cu±Fe±O±C material is believed to represent one or more surficial secondary phases, with the most obvious possibilities including a Cu±Fe carbonate (eg malachite), a Cu±Fe oxide (eg cuprous ferrite) intermixed with amorphous organic matter, or an adsorbed Cu±Fe bearing organo-metallic complex.

Secondary calcite was detected overgrowing goethite in some samples from saturated settings (plate 29), and this may be attributed to reaction of lime (CaO) derived from tailings processing with CO_2 from bacterial activity.

Although no distinctive clay morphologies or diagnostic spectra were recorded, subordinate peaks for Al, Si, Ca, Na and Mg were often recorded from thick goethite surface coatings (plate 22, Appendix 5, spectra A5.2), suggesting intimate admixtures with accessory secondary clays.

The desiccation cracks evident in plates 20 to 22 are believed to be artefacts of the sample preparation procedure, since little evidence for extensive fracturing of the iron-oxide coatings of silicate or slag fragments was evident from petrographic work. This process may have significant implications for processes which result in drying of the tailings material. Dehydration fracturing of the carapace of grains may accelerate fluid infiltration and further reaction (see Leach tests).

Grain coatings and intergranular cement of amorphous, structureless carbon was noted from IFESEM work on samples from water saturated, reduced settings in the delta. This material may be one of the products of bacterial activity.

In thin section and under the IFESEM, pyrite grains were often found to be strongly pitted. Examples of such pits are provided in plates 30 and 31. The cores of these large and small pits were identified as being dominated by iron-oxides, with the suggestion of minor sulphur (ie sulphates) indicated from X-ray spectra (Appendix 5, A5.8). It is possible that the oxidation of pyrite commences in these small holes and progresses outwards. This is supported by the thinly layered rim of iron-oxide developed on the outer margin of one of these pits (plate 32) adjacent to fresh pyrite.

Leach tests

General

Five vacuum-dried sediment samples were subjected to three single-step leach tests. Samples KR-1, DEL-WS12-S and DEL-WS3-S were taken from water saturated environments, the first from the bed of the King River, and the latter two from the delta. Samples DT-1 and H-S7 were collected from unsaturated zones on the delta and Bank H, respectively. Analytical results are presented in tables 6 to 11.

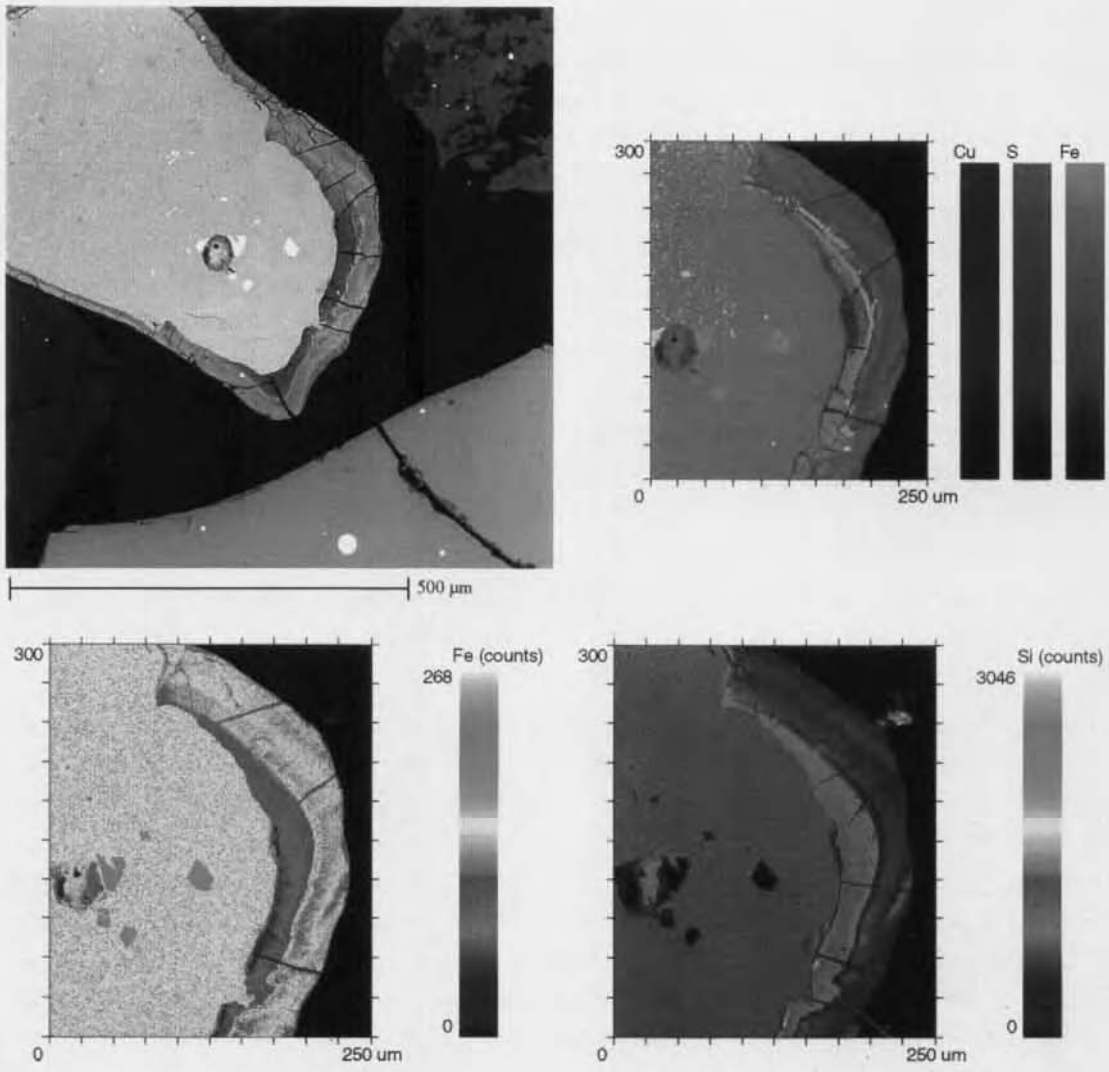

Plate 17 Sample DEL-WS5-S. Back scattered electron (BSE) (black and white) and X-ray mapping images from microprobe analysis of a slag grain. A banded hydration rim surrounding anhydrous slag is evident in the BSE image. The colour enhanced X-ray images highlight reactions associated with hydration of the margins of slag fragments. The banding evident in the BSE image, as well as in the thin section (plate 14), is reflected in multiple elemental enrichments and depletions in the X-ray maps. These patterns are not duplicated in proximal grains.

Distilled water

Single-step leach tests using distilled water on sediments from saturated and unsaturated environments demonstrated unequivocally that high concentrations of acid and metals can be released from tailings material that has been subjected to drying, with or without minor oxidation, by interaction with rainwater (tables 6 and 8). The following observations can be made:

- Interaction between the tailings sediment and distilled water generated significant acid immediately in all cases. The lowest pH was generated by samples from unsaturated environments.

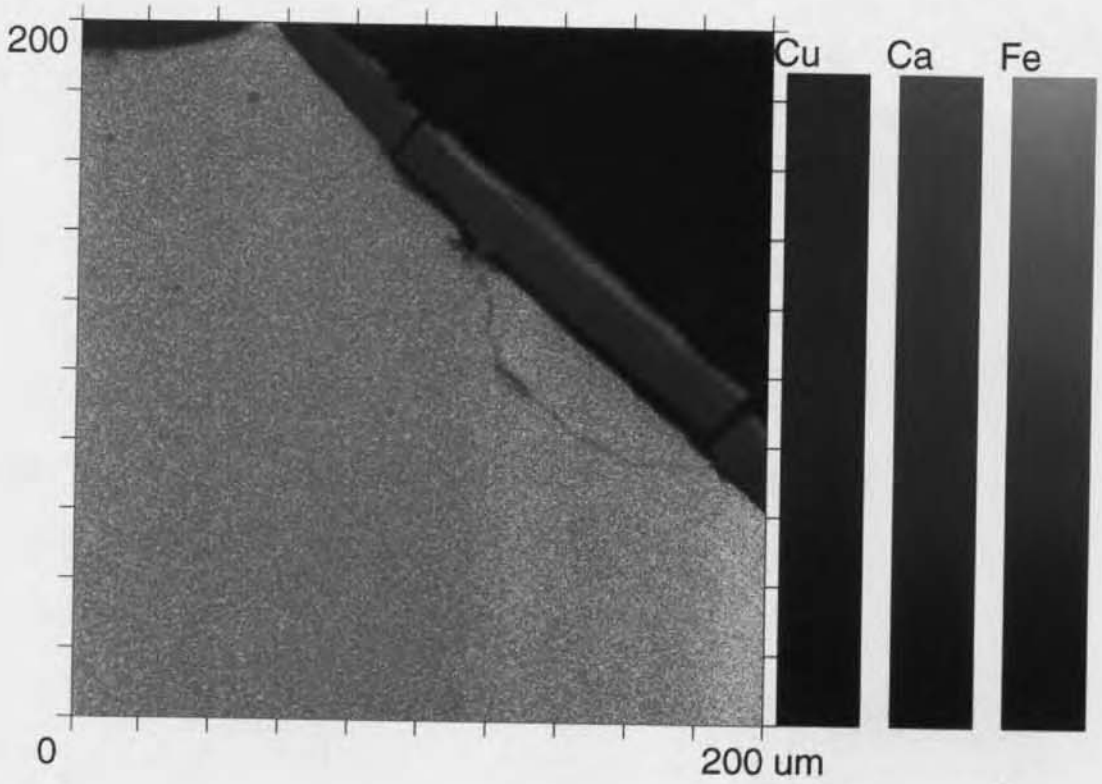

Plate 18 Sample DEL-WS5-S. X-ray mapping image from microprobe analysis of a slag fragment. Significant iron enrichment on the outer edge (red) probably reflects the development of an iron-oxide coating. An intermediate band (purple) indicates copper enrichment in the hydrated zone surrounding the anhydrous slag material (orange-brown).

- The pH of all leachates increased slightly over time, in conjunction with a significant rise in the EC. These results may indicate the influence of acid consuming dissolution reactions.
- Aqueous sulphate concentrations are not directly proportional to leachate acidity, suggesting that other processes may be responsible for at least some of the latent acidity in tailings material (see Discussion).
- The highest concentrations of most metals were derived from the slag-rich samples KR-1 (≈40 vol% slag) and DT-1 (≈15 to 20 vol% slag), strongly supporting observations regarding the high reactivity of the slag.
- Very high Cu and Zn concentrations were extracted from KR-1 (5.5, 24 mg/L respectively) and DEL-WS3-S (6.5, 5.6 mg/L respectively).
- Very high concentrations of Si, Fe and Al were extracted from all samples except DEL-WS12-S.
- Some of the elevated metals in leachate samples were not identified as significant in groundwater. For example, relatively high concentrations of Zn (up to 24 mg/L), Co (up to 16 mg/L) and Ni (3 mg/L) were recorded. These results are believed to be partly attributable to the high proportion of slag in some samples, as well as variations in redox conditions between the natural and artificial leaching processes.

Table 5 Sediment chemistry

Units	PPM	PPM	PPM	PPM	PPM	PPM	PPM	PPM	PPM	PPM	PPM	PPM	PPM	PPM	PPM	PPM	PPM	PPM	PPM	PPM	PPM	*Other Analytical Techniques
Detection limit	3	3	2	2	5	5	2	100	5	2	2	1	2	5	10	10	5	10	10	5	500	
Sample Number	As	Mo	Cr	Zn	Cd	Pb	Co	Fe	Mn	V	Cu	Ag	Ni	Bi	Ca	Mg	P	Na	K	Sn	S	
D-S-8	36	48	22	52	<5	30	<2	62400	90	77	135	<1	4	<5	125	3100	580	460	17000	15	4400	1,2
D-S-9	6	<3	26	22	<5	15	4	23300	90	29	76	<1	4	<5	680	2400	220	1200	7300	5	1700	
DEL-C1-0-10	24	34	16	220	<5	40	74	75800	400	83	1100	<1	13	<5	2100	6800	1300	580	16500	15	22800	1,2
DEL-C1-10-70	26	42	25	280	<5	70	96	74900	900	74	2400	<1	21	<5	2200	6800	860	440	15500	15	30300	
DEL-C1-70-135	38	20	30	360	<5	340	42	25400	220	26	1900	2	9	<5	1000	1400	460	880	5300	10	8100	1
DEL-C1-135-175	46	12	28	195	<5	340	30	21900	200	21	1700	1	8	<5	880	1100	500	760	3700	10	9000	1,2
DEL-C1-175-235	<3	<3	13	16	<5	5	<2	7900	60	17	7	<1	6	<5	480	2100	75	1100	6000	<5	1300	
DEL-C1-230SP	<3	<3	22	28	<5	5	3	11800	100	25	19	<1	7	<5	760	2800	115	1700	8900	<5	1600	
DEL-C1-235-250	22	4	29	195	<5	145	7	17600	145	28	260	<1	10	<5	1100	2800	160	1500	8100	10	3600	
DEL-C1-250-330	14	14	24	155	<5	80	25	25800	300	32	820	1	8	<5	1200	3000	320	980	8300	5	7400	
DEL-C1-330-365	<3	<3	25	21	<5	<5	3	9900	140	24	6	<1	8	<5	1300	3200	90	1400	6000	<5	2600	
DEL-C1-365-420	<3	<3	34	24	<5	5	4	12100	135	29	7	<1	11	<5	1100	4400	110	1700	8400	10	2600	
DEL-C1-420-550	4	<3	32	24	<5	10	4	12300	145	30	10	<1	10	<5	1200	4300	105	1600	8700	5	2500	1
DEL-S1	18	36	19	240	<5	60	49	58900	860	74	2200	<1	15	<5	2300	7100	860	1800	16300	15	16700	
DEL-S2	28	42	21	240	<5	65	81	72900	880	75	2200	<1	19	<5	2300	6700	980	520	15000	15	29300	
DEL-S3	26	42	28	280	<5	85	75	70500	900	74	2400	<1	16	<5	2400	5400	900	660	14700	20	25600	
DEL-S5	10	52	33	360	<5	85	52	51500	580	71	2600	<1	12	<5	1500	5000	700	420	14900	15	13300	
DEL-S6	14	42	27	240	<5	60	53	59600	840	69	2100	<1	13	<5	2200	6200	820	800	14900	15	17100	
DEL-S7	30	40	21	240	<5	65	105	82200	1100	80	1900	<1	20	<5	2400	6400	1000	520	15000	20	44500	
DEL-S8	12	56	40	240	<5	95	34	61700	280	64	1900	<1	8	<5	2000	4400	700	420	13200	15	9900	
DEL-S9	30	46	15	300	<5	30	105	84800	960	110	1500	<1	19	<5	4300	11200	1700	260	18000	20	33500	1,2,4
DEL-S10	36	30	14	420	<5	65	130	97300	1500	99	1400	<1	17	<5	7200	10800	2200	280	15700	20	33500	
DEL-S11	34	72	51	420	<5	95	140	110000	1000	82	4000	<1	21	<5	4500	8100	1000	620	15900	20	40500	
DEL-S27	12	36	28	145	<5	50	20	44500	220	61	1800	<1	8	<5	1000	4800	660	340	12800	15	5600	
DEL-S29	24	44	25	240	<5	65	86	71000	820	71	2200	<1	17	<5	2400	6200	920	620	14500	10	30000	
DEL-S30	20	50	22	195	<5	50	65	68400	480	80	1600	<1	15	<5	2000	6200	960	520	15600	20	20700	
DEL-S43	12	46	23	110	<5	70	7	46200	115	61	1100	<1	3	<5	740	3700	660	420	13700	15	3800	
DEL-WS3-S	18	34	18	185	<5	55	46	56000	640	61	1700	<1	10	<5	1600	5300	680	780	12800	15	22300	1,5
DEL-WS5-S	20	48	30	300	<5	100	55	64200	760	65	2300	<1	13	<5	2200	5800	700	700	14800	15	14400	1,2,4
DEL-WS8-S	38	36	34	560	<5	400	85	51500	400	41	2300	20	19	<5	2300	3300	700	720	8800	10	21400	1
DEL-WS9-S	12	57	46	340	<5	95	69	65900	1000	68	2300	<1	14	<5	2600	5500	680	560	14400	20	13100	
DEL-WS10-S	8	55	37	380	<5	90	68	65400	980	63	2800	<1	11	<5	2900	5200	680	420	13700	20	12300	
DEL-WS12-S	16	40	29	165	<5	55	66	61800	980	76	1200	<1	20	<5	2700	6500	1100	620	14700	15	25600	1,2,4,5
DEL-WS13-S	10	38	23	170	<5	45	47	57500	860	69	1300	<1	12	<5	1900	6500	660	540	17200	20	17700	
DELTA-0.0	24	38	27	400	<5	75	87	78000	900	85	2000	<1	14	<5	3400	8500	1100	860	16900	25	24800	
DELTA-10.0	26	40	26	140	<5	40	77	70300	500	68	1200	<1	17	<5	1200	6000	600	2800	15700	15	38100	
DT-1	10	89	62	220	<5	105	25	92800	145	63	1400	<1	7	<5	1500	4300	720	520	13100	15	9100	1,2,3,4,5
H-S7	38	44	21	115	<5	45	3	62700	170	90	480	<1	6	<5	780	5100	860	440	17400	15	2900	1,2,5
H-S8	32	59	21	42	<5	60	2	50600	75	72	88	<1	4	<5	80	2500	600	480	12200	15	3400	
H-W1-335	8	<3	31	21	<5	20	3	31900	95	43	89	<1	5	<5	560	2700	240	1600	9300	10	1300	
H-WD2-453	38	<3	30	240	<5	25	29	11900	100	34	340	2	16	<5	560	2200	300	1700	6400	<5	7200	2
H-WS2-355	8	<3	47	29	<5	110	12	10900	105	40	740	<1	10	<5	840	3800	900	1600	9200	10	1200	
H-W3-365	4	<3	41	33	<5	15	5	9500	100	45	10	<1	8	<5	560	3300	280	1700	12200	10	600	
KR-1	22	440	340	1500	<5	180	320	290000	520	53	5100	<1	31	<5	20300	4500	560	1200	7300	30	22000	1,2,3,4,5
N-S7	28	32	17	110	<5	35	4	49000	160	83	240	6	6	<5	800	5000	820	380	12300	20	1600	
N-S8	67	44	12	220	<5	35	240	117000	760	105	1400	<1	33	<5	3700	8500	1600	240	13200	25	77500	1
N-S9	14	38	26	165	<5	45	37	57200	440	84	840	<1	14	<5	2200	6400	1400	460	16600	15	13200	

Table 5 (continued) Sediment chemistry

Units	PPM	PPM	PPM	PPM	PPM	PPM	PPM	PPM	PPM	PPM	PPM	PPM	PPM	PPM	PPM	PPM	PPM	PPM	PPM	PPM	PPM	*Other Analytical Techniques
Detection limit	3	3	2	2	5	5	2	100	5	2	2	1	2	5	10	10	5	10	10	5	500	
Sample Number	As	Mo	Cr	Zn	Cd	Pb	Co	Fe	Mn	V	Cu	Ag	Ni	Bi	Ca	Mg	P	Na	K	Sn	S	
N-W1-486	4	<3	35	150	<5	30	5	17000	75	40	840	<1	8	<5	760	3200	240	1700	9200	10	<500	
N-W2-425	10	<3	47	94	<5	35	7	10300	75	51	500	<1	9	<5	680	3700	500	1800	11100	5	600	
N-W3-353	<3	<3	36	27	<5	15	26	9600	95	40	78	<1	17	<5	840	3700	190	1800	10300	<5	1000	
R-C1-0-20	38	32	17	120	<5	40	5	55100	150	85	155	10	8	<5	960	4900	900	400	13500	15	2600	1,2
R-C1-50-70	32	42	19	59	<5	50	2	39200	90	73	65	<1	5	<5	120	3200	480	460	13500	15	1700	
R-C1-100-120	34	48	17	62	<5	35	2	60200	100	78	100	<1	4	<5	220	3800	740	520	16500	25	3300	
R-C1-150-250	46	38	29	56	<5	50	66	54900	100	63	1500	<1	17	<5	660	3500	1100	580	13400	10	38200	
R-C1-250-280	79	40	30	420	<5	100	150	44900	100	81	1500	<1	37	<5	620	3800	1100	660	12000	10	30600	1
R-C1-330-350	22	42	32	135	<5	175	97	33700	115	52	740	1	22	<5	900	2900	800	640	9300	20	20600	
R-C1-350-370	32	42	27	125	<5	60	83	53000	110	63	740	8	19	<5	800	3400	780	460	12600	15	30400	1
R-C1-400-420	36	4	38	65	<5	130	34	16400	85	44	140	<1	14	<5	620	2800	260	1600	11500	10	4800	
R-C1-500-520	4	<3	46	31	<5	15	4	17100	140	52	56	<1	9	<5	780	3700	200	1900	12600	5	800	2
R-C1-580-600	<3	<3	30	16	<5	5	<2	28000	85	32	6	<1	5	<5	620	3100	125	1500	9400	5	1000	1
R-C1-620-640	<3	<3	26	19	<5	15	3	14200	130	30	10	<1	8	<5	660	3200	130	1400	8100	<5	<500	
R-C1-650-670	<3	<3	35	25	<5	5	3	14700	145	33	15	13	9	<5	740	3900	135	1700	10100	<5	<500	
R-C1-730-745	<3	<3	36	23	<5	<5	2	11100	90	28	25	<1	10	<5	540	3900	105	1500	10600	<5	<500	1,2
R-WD1-556	<3	<3	39	22	<5	10	4	9800	100	28	560	<1	13	<5	1200	4500	105	1700	8900	5	<500	1,2
R-WS1-489	<3	<3	29	17	<5	15	3	19600	85	36	28	<1	7	<5	760	3200	185	1700	9500	10	800	
R-W2D-700	<3	<3	40	25	<5	<5	4	11500	125	34	30	<1	14	<5	3100	5500	110	1600	9600	5	<500	
R-W2S-570	6	<3	40	29	<5	30	27	15000	120	46	52	1	12	<5	640	3300	200	1800	10900	5	1200	
R-W3-394	20	12	33	59	<5	30	14	31900	220	55	220	<1	9	<5	600	3400	580	1400	12500	10	2300	
STN-16-0.0	10	280	300	1200	<5	170	280	276000	340	41	4300	<1	9	<5	20700	3600	460	540	6300	25	20400	
STN-16-2.5	30	420	88	2300	<5	1100	500	286000	1300	57	3700	<1	31	<5	20700	4200	860	460	9200	30	32600	
STN-18-0.0	<3	440	340	1500	<5	260	280	311000	380	43	4900	<1	6	<5	23000	3700	500	520	5600	25	15800	
STN-18-2.5	28	460	97	3300	<5	1800	480	275000	360	45	3300	<1	12	<5	25800	3600	760	500	6500	35	13000	
STN-19-C-0.0	18	82	39	400	<5	100	70	73100	680	68	1900	<1	11	<5	4800	7100	780	640	14800	20	13400	
STN-19-C-6	<3	4	35	77	<5	20	5	19400	115	24	31	<1	10	<5	620	2700	135	1400	9900	<5	<500	
STN-19-L-0.0	8	340	280	1800	<5	440	240	251000	320	42	4100	<1	9	<5	18200	3600	480	580	7400	20	12700	
STN-19-L-4.4	46	165	82	10000	<5	3000	340	247000	260	45	3300	3	22	<5	28700	4100	760	680	4700	45	3600	
STN-20-C-0.0	16	69	36	480	<5	75	58	69400	640	77	2200	<1	18	<5	2900	7400	820	340	14900	20	15600	
STN-20-C-6.0	18	98	65	1300	<5	520	120	106000	240	35	1600	<1	9	<5	7300	3200	360	1000	8800	15	9600	
STN-20-R-0.0	20	53	32	380	<5	70	72	72500	740	85	2700	<1	15	<5	3100	8400	880	360	17400	20	18700	
STN-20-R-3.0	46	125	81	1600	<5	660	260	144000	420	54	3200	1	29	<5	7500	4700	560	1200	10300	30	64500	

* Legend

1. Microscopy
2. XRD
3. Microprobe
4. IFESEM
5. Leach Tests

Table 6 Analytical results from distilled water leach

Sample Number	KR-1	DT-1	DEL-WS12-S	DEL-WS3-S	H-S7	Matrix Blank	Detection Limit
Lab No.	1126	1127	1128	1129	1130		
As	12	1.2	2.5	6.3	0.4	0.3	0.2
Sn	<2.0	<2.0	<2.0	<2.0	<2.0	<2.0	2.0
Mo	2	<0.5	38	<0.5	<0.5	<0.5	0.5
Cr	<10	<10	<10	<10	<10	<10	10
Zn	24000	1600	60	5600	400	<0.1	0.1
Cd	2.5	1	1	9	<0.5	<0.5	0.5
Pb	8	8	<1	43	5	<1	1
Ba	29	28	94	27	38	<1	1
Co	16000	360	29	860	25	<0.2	0.2
Fe	6700	30000	70	14000	29000	<30	30
SiO2	45000	4600	7000	41000	24000	<1000	50
B	70	240	110	290	80	<50	100
Mn	7100	2100	13000	34000	1300	10	10
V	<20	<20	<20	<20	<20	<20	20
Cu	5500	1700	40	6500	310	<0.2	0.2
La	22	41	0.4	92	11	<0.1	0.1
Ni	3000	110	7	100	20	<0.1	0.1
Y	5.1	11	0.2	51	7.6	<5	5
Al	750	16000	150	21000	6000	<0.1	0.1
Sr	440	340	180	490	88	<10	10
Ag	<0.1	<0.1	0.1	0.1	<0.1	<0.1	0.1
SO4, mg/L	320	640	250	1100	270	<1	1

Results expressed as ug/L unless otherwise specified.

Table 7 Analytical results from dilute sulphuric acid leach

Sample Number	KR-1	DT-1	DEL-WS12-S	DEL-WS3-S	H-S7	Matrix Blank	Detection Limit
Lab No.	1126	1127	1128	1129	1130		
As	7.7	1.0	1.5	5.8	1.6	<0.2	0.2
Sn	2.0	2.0	2.0	2.0	2.0	2.0	2.0
Mo	2.5	1.0	1.5	1.0	1.0	<0.5	0.5
Cr	<10	<10	10	<10	<10	<10	10
Zn	21000	3000	860	6000	860	<0.1	0.1
Cd	4.0	1.0	2.0	6.0	0.5	<0.5	0.5
Pb	64	33	13	69	5.0	<1	1
Ba	29	25	18	19	25	<1	1
Co	7000	330	270	550	28	<0.2	0.2
Fe	26000	25000	2000	26000	26000	<30	30
SiO2	35000	81000	8200	52000	52000	<50	50
B	290	670	110	380	180	<50	100
Mn	4500	1100	20000	29000	1300	10	10
V	<20	<20	<20	<20	<20	<20	20
Cu	20000	3900	480	19000	2200	<0.2	0.2
La	130	58	8.1	140	80	<0.1	0.1
Ni	1700	25	25	72	25	<5	0.1
Y	43	21	5.1	88	110	<5	5
Al	14000	34000	2400	77000	47000	<5	0.1
Sr	310	250	150	330	170	<10	10
Ag	<0.1	0.2	<0.1	<0.1	0.1	<0.1	0.1
SO4, mg/L	1500	1700	1700	2100	1600	1600	1

Results expressed as ug/L unless otherwise specified.

- The highest Fe concentrations were associated with the most acid leachates, being derived from the two samples from unsaturated settings. At the pH indicated in table 8, the high Fe concentrations in most leachates (up to 30 mg/L) suggest the predominance of ferrous aqueous species.
- The highest Mn concentrations are associated with sediments from saturated environments, and may reflect rapid dissolution of residual manganiferous siderite (carbonate) which is not present in most unsaturated sediment samples.
- The highest EC readings were found in water saturated samples from the delta. It is most likely that relatively salt-rich pore water trapped in original samples is responsible.

Dilute sulphuric acid

Similar trends recorded for the water leach tests were found with dilute sulphuric acid extractions. The results (tables 7 and 9) show that:

- very high concentrations of metals can be mobilised by low pH fluids, in particular Fe, Si, Al, Cu, Zn, Co, Mn and Ni;
- dilute acid is more effective at dissolving metals than water, although some inconsistencies were observed. Higher Co, Zn and Ni concentrations in leachate from the water tests compared with the acid leachates suggests that sediment samples in the latter trials contained lower abundances of slag. This may be due to density separation of samples in transit and incomplete mixing at the laboratory;
- the pH of all leachates increased significantly over time, in conjunction with a general decrease in the EC. It is possible that the precipitation of iron-oxide in association with acid consuming reactions may be partly responsible for this trend;
- the lowest pH values were generated by samples from unsaturated environments, reflecting the trends observed with the water leaches;
- the highest concentrations of Cu, Zn and Co were again derived from the slag-rich sample KR-1;
- the highest Mn concentrations remain strongly associated with sediments from saturated environments; and
- similar iron concentrations (26 mg/L) were observed from all samples except DEL-WS12-S, and these values were broadly comparable with those from the water leaches. Aqueous Al values were significantly higher than for the water leach, often by a factor of 10.

Ammonium acetate

Ammonium acetate was used as a cation exchange extractant, designed to displace metals that were adsorbed to grain surfaces. Aqueous concentrations from this series of leaches cannot be directly compared with the water and acid leaches since the solid:fluid weight ratio was 5 times lower. Results (tables 10 and 11) indicate that:

- very little metal, including copper, occurs as adsorbed species on grain surfaces. Expressed as the proportion of total copper in the samples, the adsorbed component in the leach samples varies from 0.01 to 0.57 wt%. Similar ranges were evident for Mn, Co, and Zn (0.1 to 4 wt%);
- the largest concentration of adsorbed Cu, Zn, Co and Ni were mobilised from the slag-rich saturated sample KR-1. It is not known whether this can attributed to adsorption processes alone, since the reactivity of altered slag with the extractant has not been established;

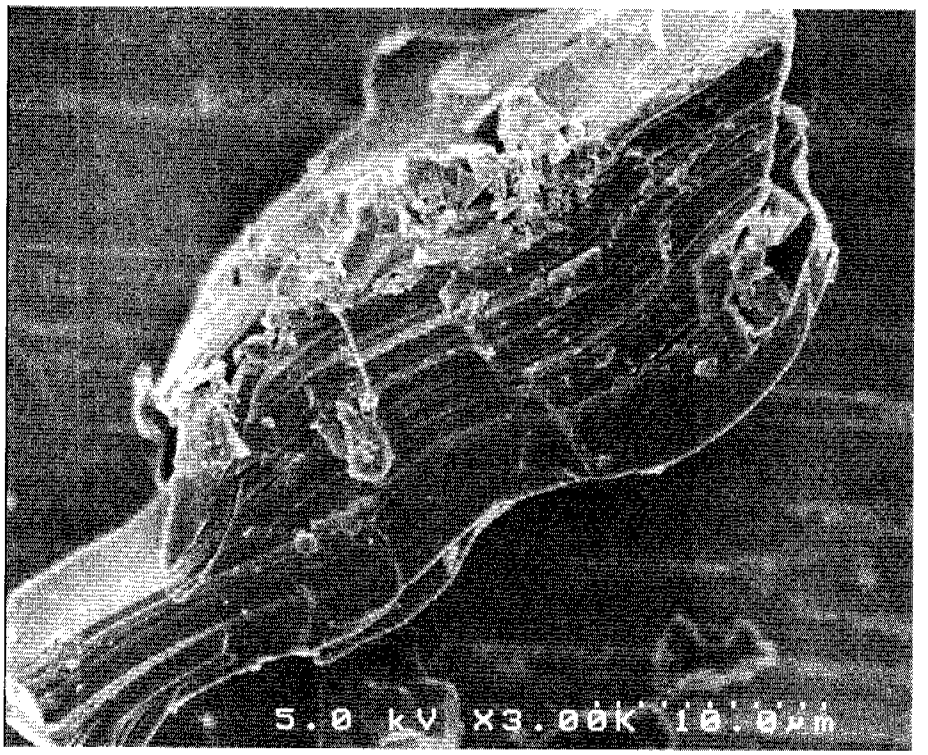

Plate 19 Sample DEL-WS12-S. IFESEM photomicrograph of a portion of the intricately layered hydration bands surrounding a slag fragment. Microprobe data in Appendix 4 (analyses A4.9 to A4.15) and spectra 1 in Appendix 5 provide an indication of the bulk composition of this material.

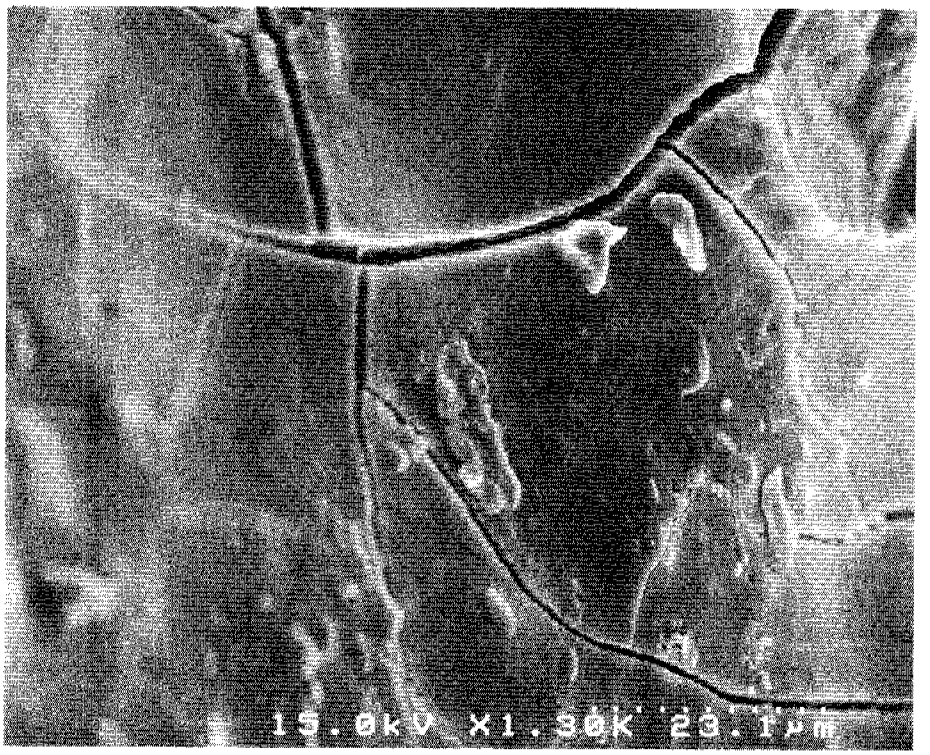

Plate 20 Sample DT-1. IFESEM photomicrograph of the typical surface appearance of a hydrated slag grain. Dessication cracks are a function of the sub-aerial setting for sample DT-1. Surface coatings of iron-oxide are not evident at this scale.

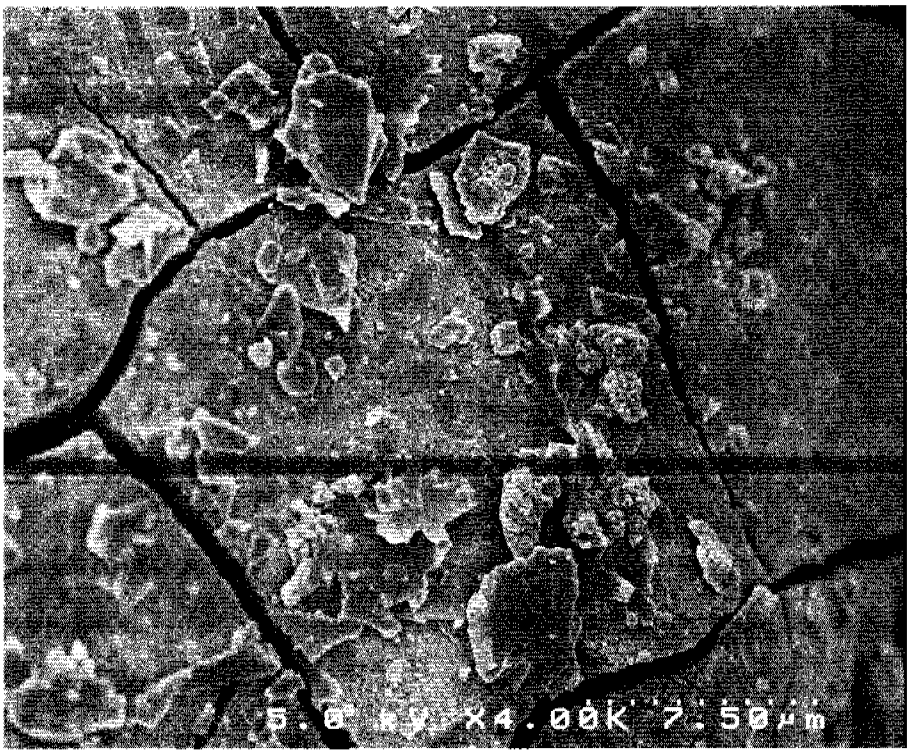

Plate 21 Sample DT-1. IFESEM photomicrograph of the iron-oxide coated surface of a grain of slag.

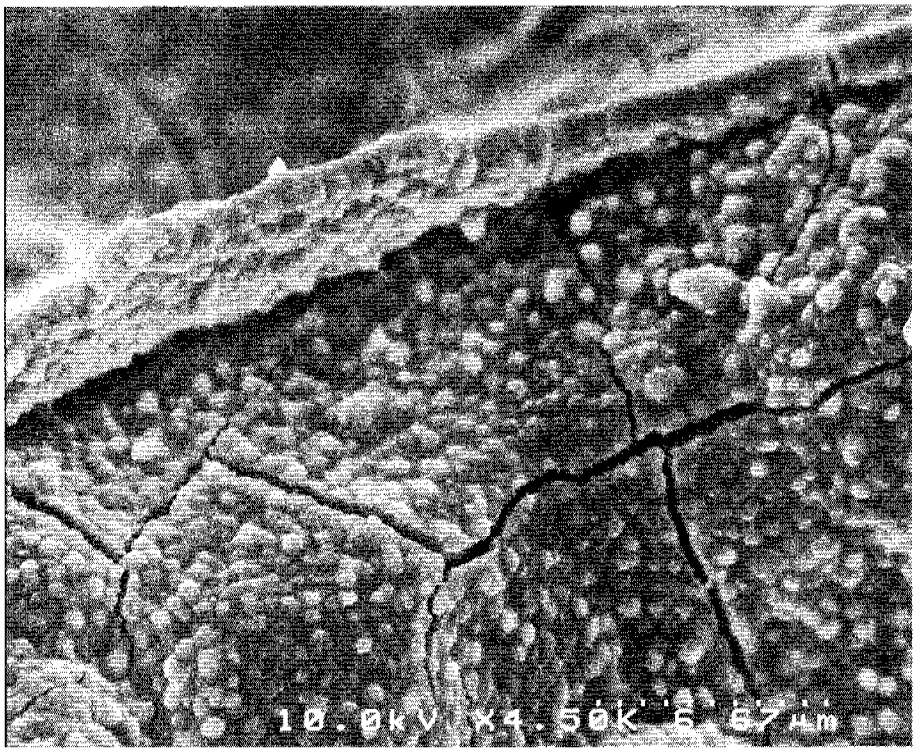

Plate 22 Sample DT-1. IFESEM photomicrograph of the iron-oxide crust around a detrital grain. Spectra 2 in Appendix 5 highlights the presence of significant copper and carbon associated with the iron and oxygen. Other peaks (aluminium, silicon, magnesium ± iron) are attributed to minor precipitation of secondary clays associated with the iron-oxide.

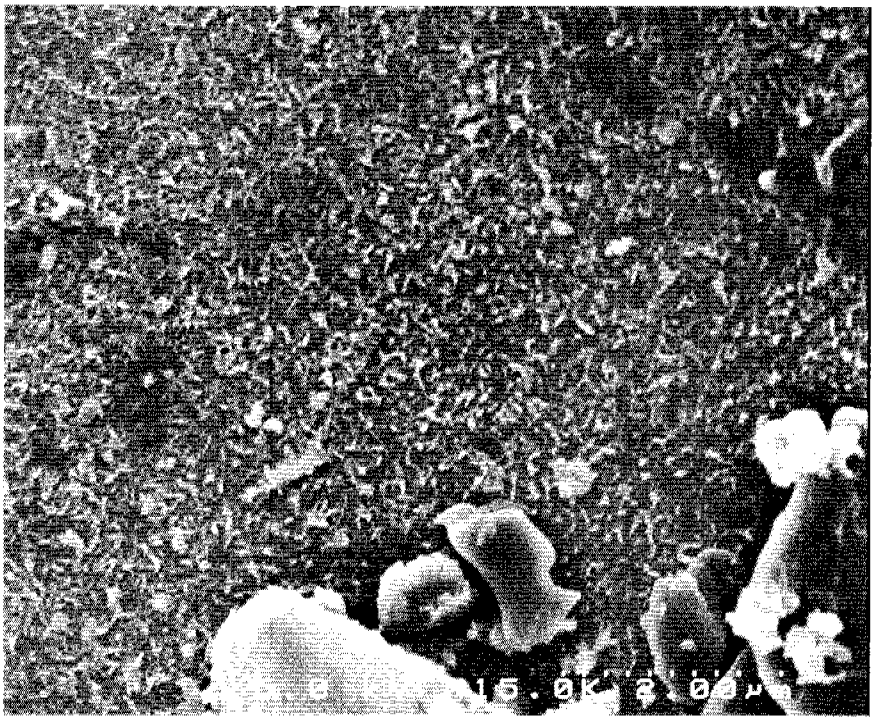

Plate 23 Sample DEL-S9. IFESEM photomicrograph of fine bladed aggregates of iron-oxide covering the flat surface of a chlorite crystal. Spectra 3 in Appendix 5 displays the iron and oxygen peaks of the iron-oxide, the copper and carbon peaks of a compound overlying and/or mixed with the iron-oxide, and the lesser peaks of the chlorite substrate. (NB. The sulphur peak overlaps with a secondary platinum peak.)

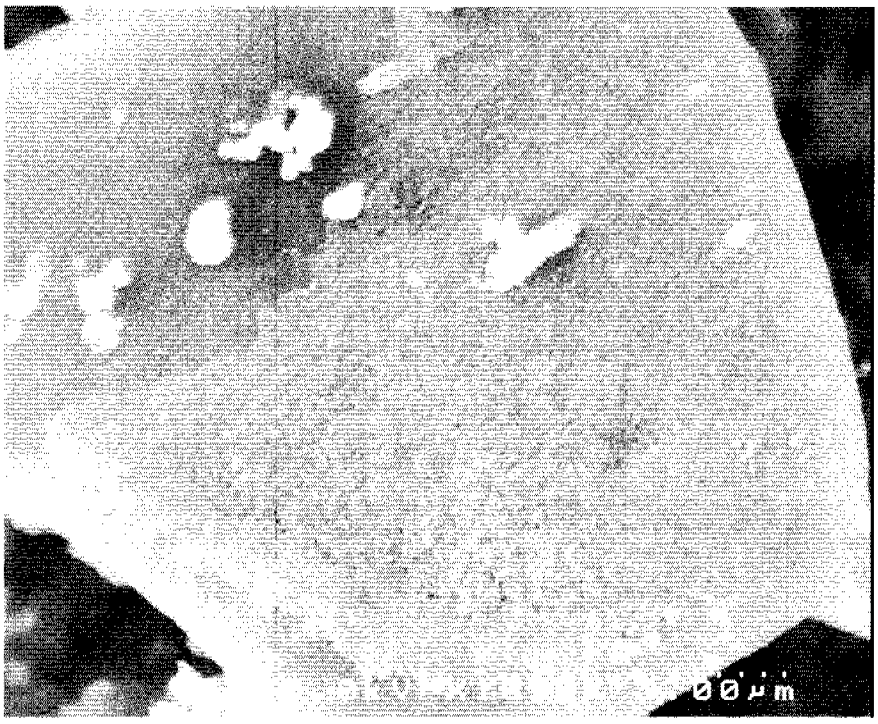

Plate 24 Sample DEL-WS5-S. IFESEM photomicrograph of a platelet of chlorite (dark-grey) partially coated with a thin (<0.3 μm) uniform veneer of iron-oxide crystals (lighter grey). No copper or carbon were detected in the top left portion of the sample, and strong peaks for iron and oxygen and lesser peaks for copper and carbon were detected over the coated zone.

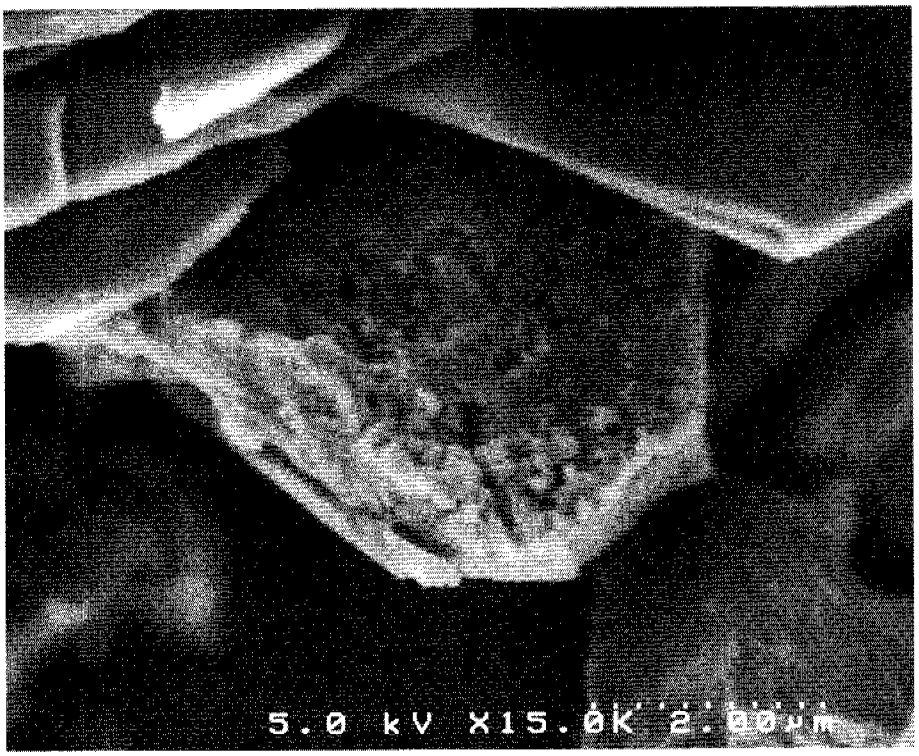

Plate 25 Sample DEL-WS12-S. IFESEM photomicrograph of several chlorite platelets. Central crystal displays an irregular coating dominated by iron, oxygen, copper and carbon (Appendix 5, spectra 4).

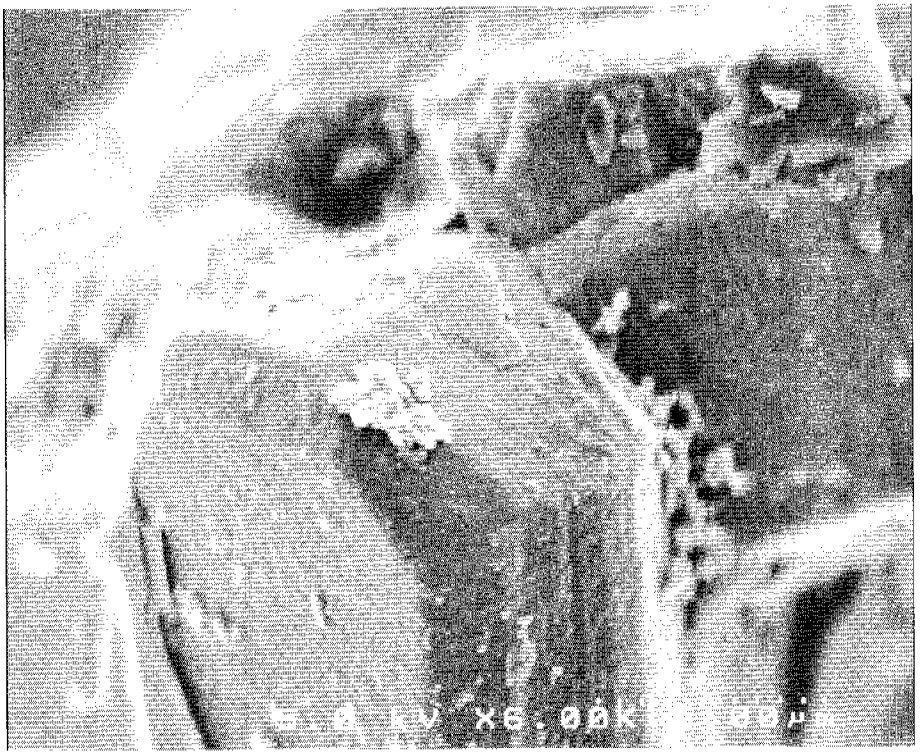

Plate 26 Sample DEL-WS12-S. IFESEM photomicrograph of detrital pyrite aggregate with an euhedral termination. The felted surface appearance is due to a thin uniform veneer of iron-oxide and sporadically distributed patches of secondary clay material. Spectra 5 in Appendix 5 displays iron, sulphur and oxygen as the major peaks, with subordinate but prominent copper and carbon peaks.

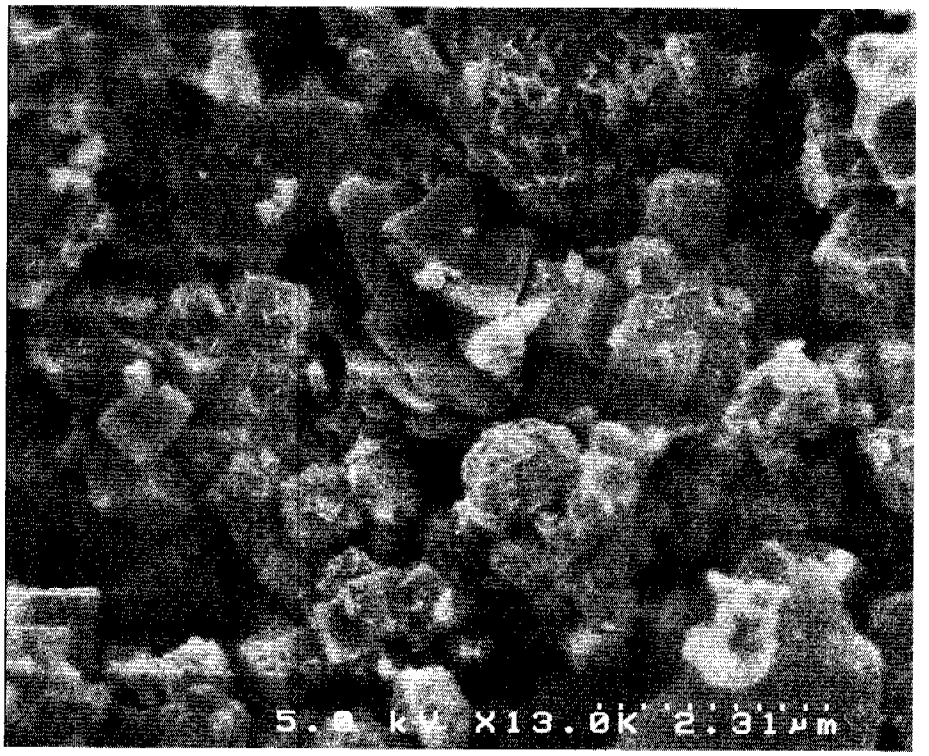

Plate 27 Sample D-S8. IFESEM photomicrograph showing masses of iron-oxide blades developed over the surface of a silicate rock fragment containing quartz and chlorite. Spectra 6 in Appendix 5 exhibits major iron, oxygen and silicon peaks and subordinate but prominent carbon and copper peaks.

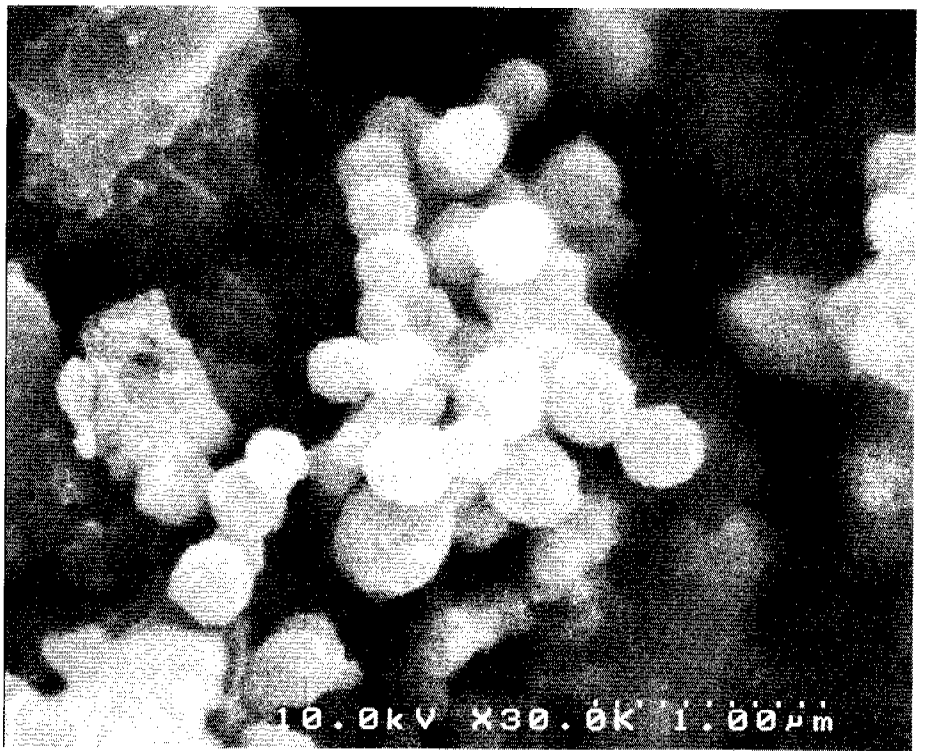

Plate 28 Sample DEL-WS5-S. IFESEM photomicrograph of spherical concentrations of iron-oxide blades developed on a chloritic substrate. Analysis of this field of view revealed major peaks for iron, oxygen and carbon and lesser peaks for copper and those representing the other components of chlorite (Appendix 5, spectra 7).

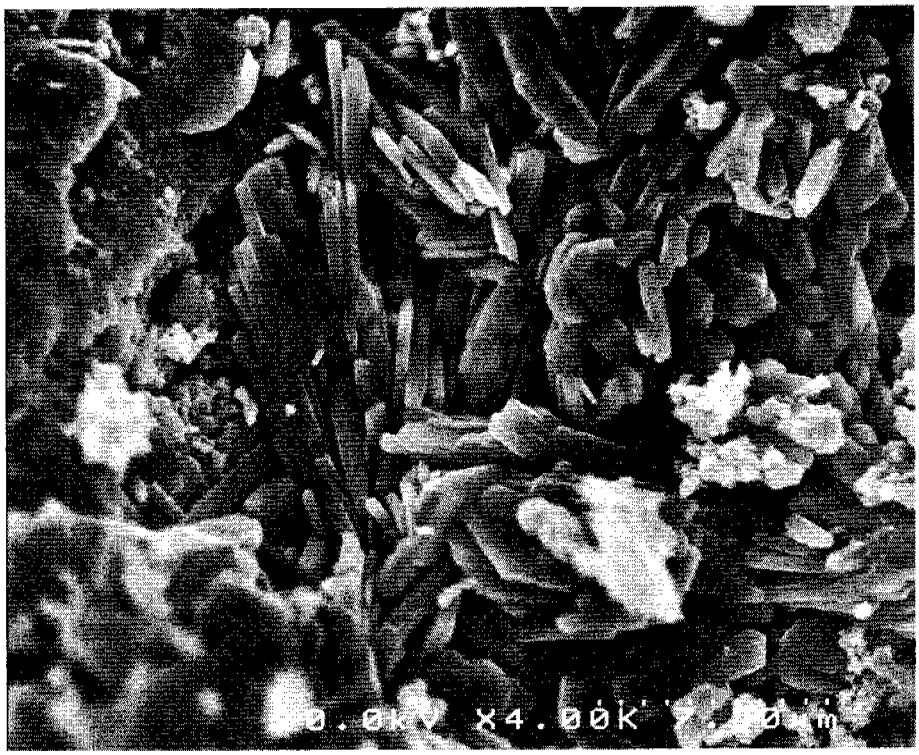

Plate 29 Sample DEL-WS5-S. IFESEM photomicrograph of euhedral masses of bladed pure calcite crystals overgrowing an iron-oxide surface coating.

- the pH, EC and Eh of the leachate remained essentially constant throughout for all samples except H-S7, where some elevated EC values were recorded; and
- the results for Cu suggest that the Cu±Fe±O±C matter on grain surfaces identified from IFESEM work is likely to be a precipitate, rather than an adsorbed compound.

Sources of metals in groundwater

The source of aqueous copper is mainly detrital chalcopyrite (≈85 to 95 wt%) and surface coatings of Cu±Fe±O±C precipitates on detrital grains (≈1 to 10 wt%). The proportions are based on the assumption that all Cu released during acid leaches was from surficial Cu-bearing precipitates. Lesser contributions may be from Cu-Fe sulphide blebs in slag fragments, copper in silicate slag, and minor amounts in accessory primary sulphides and biogenic chalcopyrite.

Iron probably comes from chlorite, pyrite, siderite, goethite, chalcopyrite, Cu-Fe sulphide blebs in slag fragments, iron-silicate slag and magnetite. Smaller contributions may come from other sulphides such as sphalerite, as well as ilmenite and chromite. Goethite, chlorite, magnetite, sphalerite, ilmenite and chromite are unlikely to contribute significantly to soluble iron concentrations, but water chemistry is predicted to be strongly influenced by the other assemblages.

Aluminium is present in silicates such as chlorite, muscovite, pyrophyllite, biotite, feldspar, spinel and slag. Since the most Al-rich groundwater is found in the banks, slag is not a primary source. Alteration of chlorite and possibly muscovite are implicated in the elevated concentrations of aqueous aluminium in groundwater from both the banks and delta.

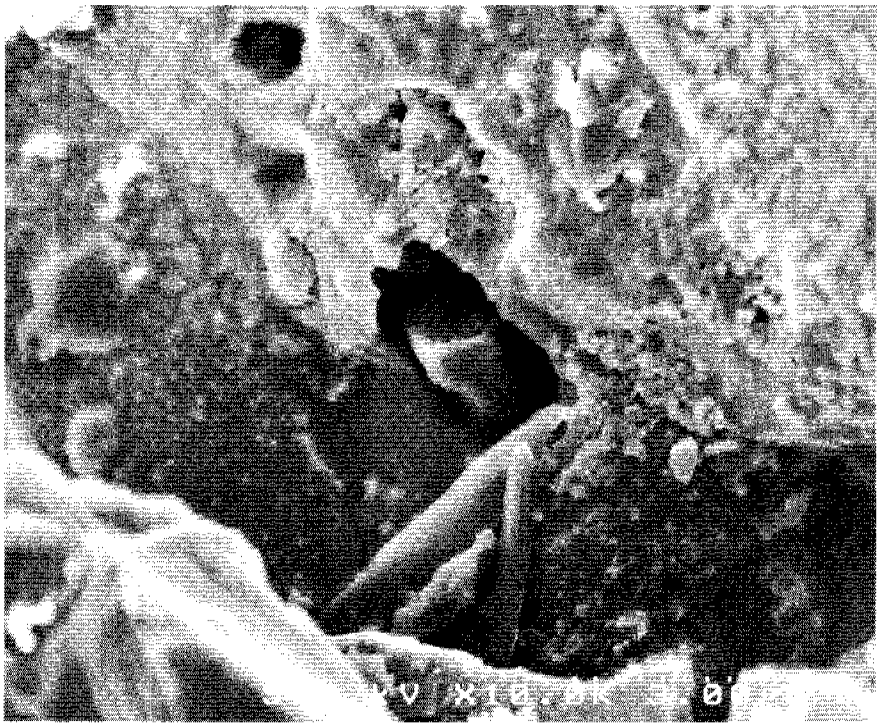

Plate 30 Sample DEL-WS12-S. IFESEM photomicrograph showing small pits in the surface of a pyrite crystal which has a widespread coating of iron-oxide. The small pits contain iron-oxide only. These pits may be instrumental in the initiation of pyrite oxidation.

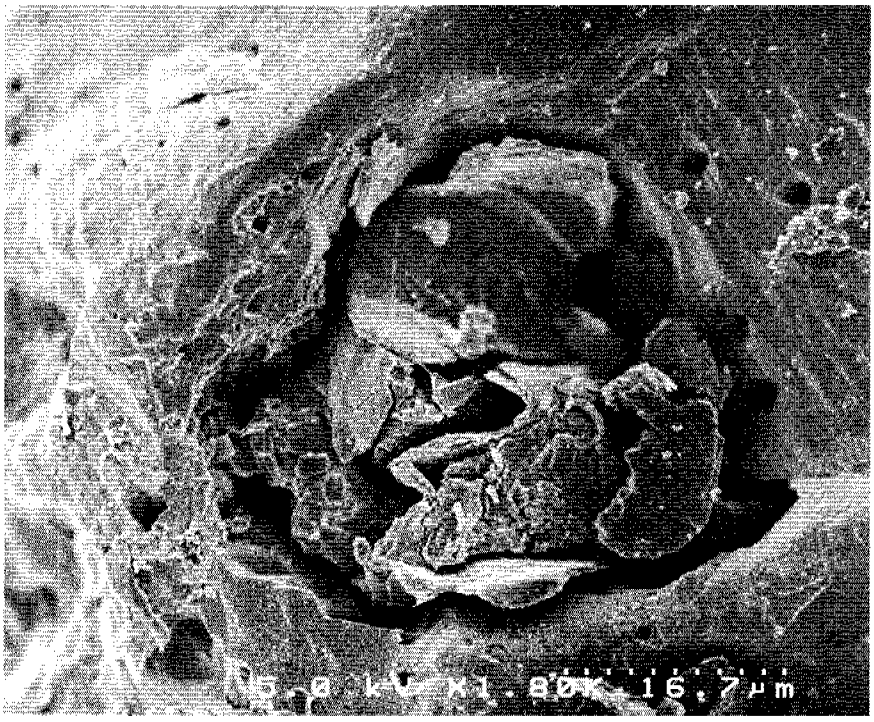

Plate 31 Sample DEL-WS12-S. IFESEM photomicrograph of a large pit surrounded by several smaller pits in a pyrite grain. Spectra 8 (Appendix 5) represents the mass of material in the large central hole. It is dominated by iron and oxygen with well defined, abeit lesser peaks for carbon, copper and sulphur. The material is considered to be largely iron-oxide with the possibility of a small component of some iron-sulphate phase. The copper and carbon are believed to be intimately associated with the iron-oxide.

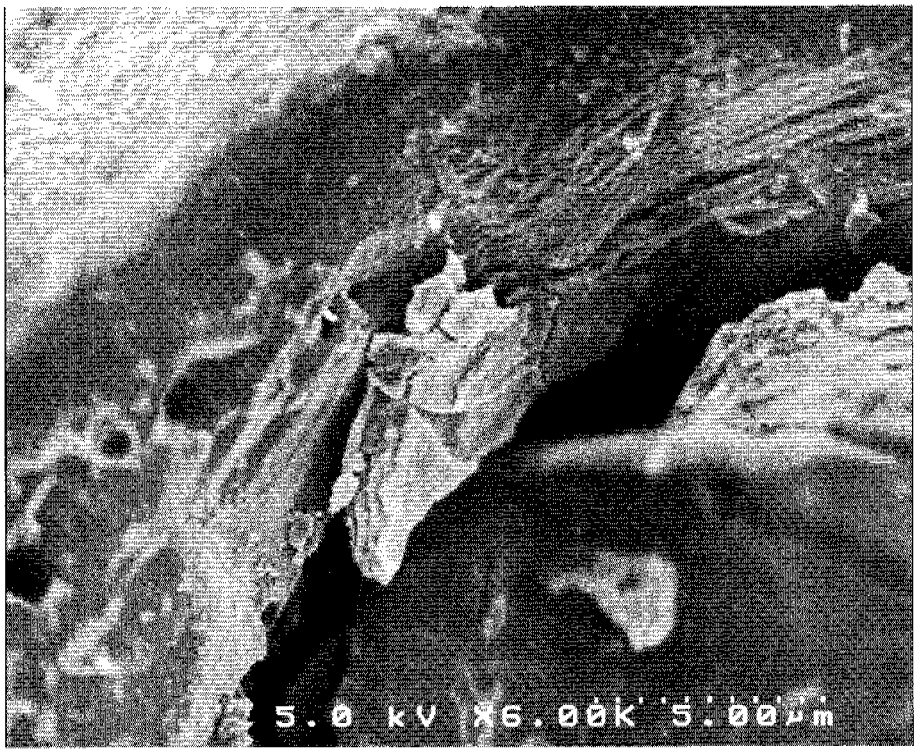

Plate 32 Sample DEL-WS12-S. IFESEM photomicrograph of an enlargement of upper-central portion of the previous plate displaying the outer margin of the large hole in a pyrite crystal. The banded material on the edge of the pit is dominated by iron-oxide, with little evidence of any suphur.

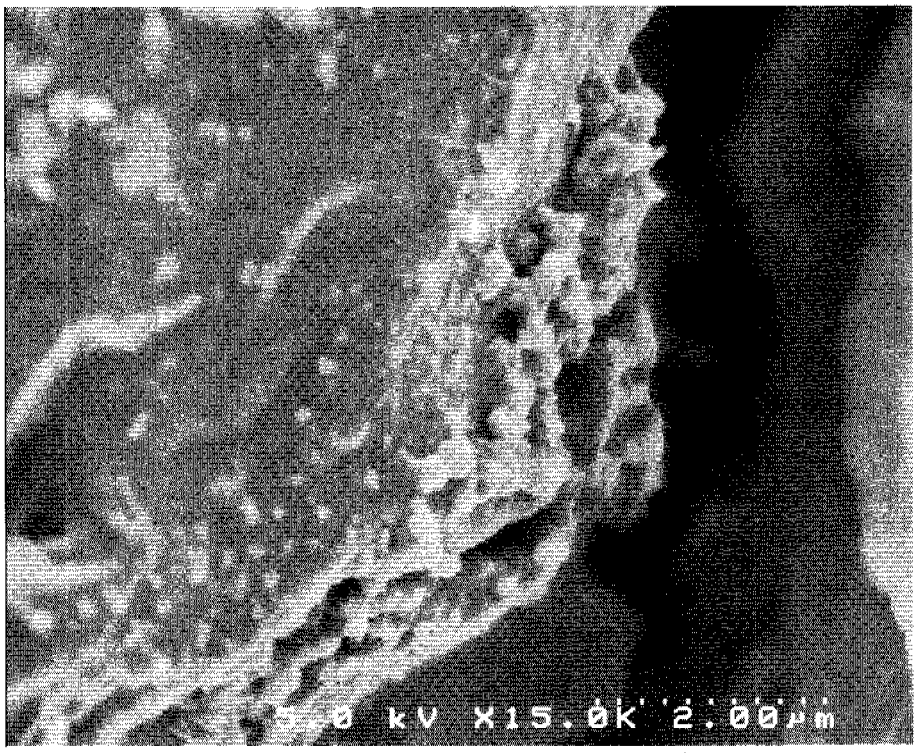

Plate 33 Sample DEL-WS12-S. IFESEM photomicrograph of an enlargement of the central-left portion of plate 31. Nodular aggregates of iron-oxide in the central region give way to dominantly fresh pyrite, with a thin coating of iron-oxide in the upper-left quadrant. Spectra 9 (Appendix 5) taken from the latter region displays iron, sulphur and oxygen peaks with lesser carbon and some indication of copper.

Table 8 pH and conductivity results from the distilled water leach

Conductivity

Sample Number	KR-1	DT-1	DEL-WS12-S	DEL-WS3-S	H-S7	Matrix Blank
Lab No.	1126	1127	1128	1129	1130	
5 min	300	660	1200	1900	390	2.00
1 hr	410	890	1300	2000	450	2.00
2 hrs	450	890	1300	2000	450	2.00
22.5 hrs	590	930	1300	2200	480	6.00
24 hrs	550	920	1400	2200	480	6.00
26hrs	550	900	1300	2100	470	6.00
28hrs	620	960	1400	2200	410	6.00
47hrs	640	1000	1400	2300	620	9.00
48hrs	640	1000	1400	2200	610	9.00

Results expressed as uS/cm unless otherwise specified.

pH

Sample Number	KR-1	DT-1	DEL-WS12-S	DEL-WS3-S	H-S7	Matrix Blank
Lab No.	1126	1127	1128	1129	1130	
5 min	4.6	2.9	6.0	3.6	3	5.8
1 hr	4.7	2.8	6.2	3.8	3.1	5.8
2 hrs	4.7	2.9	6.2	4.0	3.2	5.7
22.5 hrs	4.7	3	6.1	3.8	3.3	5.9
24 hrs	4.6	3	6.2	3.8	3.3	5.9
26hrs	4.7	3.01	6.2	3.9	3.2	5.9
28hrs	4.7	3.5	6.2	3.9	3.6	6.0
47hrs	4.7	3.5	6.8	4.0	3.6	5.8
48hrs	4.7	3.5	6.8	4.0	3.6	5.9

Results expressed as units unless otherwise specified.

Sulphur occurs in a wide range of assemblages, including pyrite, chalcopyrite, sphalerite, galena, sulphide phases in slag, sulphur in the slag, bornite (possibly in covellite and chalcocite) and barite. With the exception of barite, sphalerite and galena, all of these phases will contribute significantly to aqueous sulphur concentrations. Brackish harbour water may also be a source of sulphur, as sulphate ions, to groundwater in the delta.

The vast majority of manganese is hosted by manganiferous siderite (oligonite $Fe,Mn(CO_3)_2$); solid solution between siderite ($FeCO_3$) and rhodochrosite ($MnCO_3$), with minor contributions from slag, and possible additions from trace concentrations in pyrite. The relatively high aqueous concentrations of manganese are believed to be primarily due to the low pH of groundwater and surface water, and the high solubility of carbonates under acid conditions.

Cobalt, nickel and arsenic are predicted to be largely present as trace components in pyrite, and will be released during pyrite oxidation. Cobalt and nickel are also found in elevated concentrations in slag, from which they may be readily released. Cadmium is probably present as a trace substitute for zinc in sphalerite, and the chromium in chromite and, to a lesser extent, fuchsite (chromium-muscovite). The low solubility of these elements is likely to influence aqueous metal concentrations. Zinc occurs principally in sphalerite, and lead is dominantly in galena, although significant contributions from slag are possible. Neither

sphalerite nor galena appear to be as soluble as pyrite, and therefore aqueous zinc and lead concentrations in groundwater are relatively low.

Barium will be present primarily in barite and as a trace element in feldspar. Though barite is largely insoluble, feldspar will be reasonably reactive in acidic environments.

Selenium is a common trace element in chalcopyrite and this is probably its primary source. Aqueous selenium concentrations appear to be influenced by redox state, with reducing conditions favouring enhanced solubilities. This may be an artefact of a limited data set. The sources of mercury, antimony and thallium in groundwater are unknown, but are assumed to be tailings related.

The major component of the tailings is silica, which is derived from quartz, assorted aluminosilicates (chlorite, muscovite, biotite, feldspar) and slag. In general, Si concentrations in groundwater are close to saturation with respect to microcrystalline quartz (refer to geochemical modelling). Sodium, potassium and chloride in groundwater are largely supplied by brackish harbour water. Calcium and magnesium are also largely from harbour water, with lesser contributions from carbonates (eg calcite, dolomite and siderite), lime and possibly chlorite.

Table 9 pH and conductivity results from the dilute sulphuric acid leach

Conductivity

Sample Number	KR-1	DT-1	DEL-WS12-S	DEL-WS3-S	H-S7	Matrix Blank
Lab No.	1126	1127	1128	1129	1130	
5 min	2500	3600	2500	4300	4700	5800
1 hr	2200	3600	2500	4300	4400	6800
2 hrs	1800	3200	2500	3900	4100	6700
5 hrs	1700	2600	2600	3500	3100	6500
16 hrs	1900	2600	3400	4100	2500	7600
19 hrs	1600	2100	2600	3300	2100	6900
23 hrs	1700	2100	2600	3500	2100	6900
39 hrs	1700	2000	2600	3400	2000	6900
45 hrs	1800	2000	2800	3500	2000	6700
48 hrs	1700	1900	2700	3400	2000	6600

Results are expressed as uS/cm unless otherwise specified.

pH

Sample Number	KR-1	DT-1	DEL-WS12-S	DEL-WS3-S	H-S7	Matrix Blank
Lab No.	1126	1127	1128	1129	1130	
5 min	2.2	2	2.3	2.1	2	1.8
1 hr	3.2	2.3	3.9	2.6	2.2	2.0
2 hrs	3.3	2.3	4	2.6	2.2	2.1
5 hrs	3.5	2.5	4.3	3.0	2.4	2.1
16 hrs	3.6	2.5	4.5	3.1	2.2	1.8
19 hrs	3.6	2.6	4.5	3.2	2.4	1.8
23 hrs	3.6	2.7	4.7	3.1	2.4	1.8
39 hrs	3.9	3.2	5.2	3.4	2.9	2.1
45 hrs	3.9	3.2	5.3	3.4	3	2.2
48 hrs	3.9	3.2	5.4	3.3	2.9	2.2

Results are expressed as units unless otherwise specified.

Table 10 Analytical results from ammonium acetate leach

Sample Number	KR-1	DT-1	DEL-WS12-S	DEL-WS3-S	H-S7	Matrix Blank	Detection Limit
Lab No.	1126	1127	1128	1129	1130		
As	2.6	0.3	0.6	0.7	0.9	<0.2	0.2
Sn	<2.0	<2.0	<2.0	<2.0	<2.0	<2.0	2.0
Mo	8	0.5	9.2	0.7	11.0	<0.5	0.5
Cr	<10	<10	<10	<10	<10	<10	10
Zn	2900	47	240	93	220	<0.1	0.1
Cd	1.2	<0.5	1.9	0.8	37	<0.5	0.5
Pb	8	4	35	27	19.0	<1	1
Ba	2000	350	1600	510	1000	<1	1
Co	2300	3.8	110	35	2.1	<0.2	0.2
Fe	<30	<30	<30	<30	<30	<30	30
SiO2	5600	8200	800	800	10000	<50	50
B	<50	<50	<50	<50	<50	<100	100
Mn	900	<10	4000	1100	<10	<10	10
V	<20	<20	<20	<20	<20	<20	20
Cu	2900	14	590	940	140	<20	0.2
La	24	1.6	2.2	3.5	210	<0.1	0.1
Ni	530	<5	<5	<5	<5	<0.1	0.1
Y	5.5	0.2	1.1	1.6	1.1	<5	5
Al	110	<10	30	<10	10	<0.1	0.1
Sr	300	61	130	81	36	<10	10
Ag	<0.1	0.1	3	<0.1	0.2	<0.1	0.1
SO4, mg/L	72	570	55	140	140	<1	1

Results expressed as ug/L unless otherwise specified.

6 Modelling

6.1 Hydrogeology

Parameters for groundwater flow modelling

Hydraulic conductivity values were calculated from water level recovery tests performed on many of the piezometers after sampling. Data from Banks R, N and H were analysed using the Hvorslev recovery test method for an unconfined, partially-penetrating well (Hvorslev 1951). The hydraulic conductivity of the sediments around each well was assumed to be isotropic for the purpose of the Hvorslev analysis (table 12). In Bank D and the north and south lobes of the delta, where recovery rates of water levels were too rapid to measure by hand, a minimum hydraulic conductivity value was estimated based on the amount of groundwater removed and a recovery time of about 20 s. Results and equations used are included in table 12. Data used to determine the value T_0 (see table 12) for each Hvorslev analysis are included in table 13 and figure 25.

Hydraulic conductivity values of sediments in the higher banks, Banks H, N and R, were significantly lower ($K = 7x10^{-8}$ to $1x10^{-6}$ m/s; table 12) than those estimated for sediments further downstream, Bank D and the north and south lobes of the delta ($K \approx 1x10^{-4}$ m/s, table 12). Some of the variation in hydraulic conductivity values measured in the higher banks is probably due to smearing of clay particles in the monitoring interval during drilling. This would reduce the apparent hydraulic conductivity of the sediments immediately surrounding the